Published in final edited form as:

J Am Coll Cardiol. 2018 June 05; 71(22): 2511–2522. doi:10.1016/j.jacc.2018.02.079.

Coronary Atherosclerotic Precursors of Acute Coronary Syndromes

Hyuk-Jae Chang, MD, PhD[1], **Fay Y. Lin, MD**[2], **Sang-Eun Lee, MD, PhD**[1], **Daniele Andreini, MD, PhD**[3], **Jeroen Bax, MD, PhD**[4], **Filippo Cademartiri, MD, PhD**[5], **Kavitha Chinnaiyan, MD**[6], **Benjamin J.W. Chow, MD**[7], **Edoardo Conte, MD**[3], **Ricardo C. Cury, MD**[8], **Gudrun Feuchtner, MD**[9], **Martin Hadamitzky, MD**[10], **Yong-Jin Kim, MD**[11], **Jonathon Leipsic, MD**[12], **Erica Maffei, MD**[13], **Hugo Marques, MD**[14], **Fabian Plank, MD**[9], **Gianluca Pontone, MD, PhD**[3], **Gilbert L. Raff, MD**[6], **Alexander R. van Rosendael, MD**[4], **Todd C. Villines, MD**[15], **Harald G. Weirich, MD**[9], **Subhi J. Al'Aref, MD**[2], **Lohendran Baskaran, MD**[2], **Iksung Cho, MD**[1,2,16], **Ibrahim Danad, MD**[17], **Donghee Han, MD**[1,2], **Ran Heo, MD**[18], **Ji Hyun Lee, MD**[1,2], **Asim Rivzi, MD**[2,19], **Wijnand J. Stuijfzand, MD**[2], **Heidi Gransar, MSc**[20], **Yao Lu, MSc**[2], **Ji Min Sung, PhD**[1], **Hyung-Bok Park, MD**[1], **Daniel S. Berman, MD**[20], **Matthew J. Budoff, MD**[21], **Habib Samady, MD**[22], **Leslee J. Shaw, PhD**[22], **Peter H. Stone, MD**[23], **Renu Virmani, MD**[24], **Jagat Narula, MD, PhD**[25], and **James K. Min, MD**[2]

[1]Division of Cardiology, Severance Cardiovascular Hospital, Integrative Cardiovascular Imaging Research Center, Yonsei University College of Medicine, Seoul, South Korea [2]Dalio Institute of Cardiovascular Imaging, Department of Radiology, NewYork-Presbyterian Hospital and Weill Cornell Medicine, New York, New York [3]Department of Clinical Sciences and Community Health, University of Milan, Centro Cardiologico Monzino, IRCCS Milan, Italy [4]Department of Cardiology, Heart Lung Center, Leiden University Medical Center, Leiden, the Netherlands [5]Cardiovascular

Address for correspondence: James K. Min, MD, Dalio Institute of Cardiovascular Imaging, New York-Presbyterian Hospital and Weill Cornell Medical College, 413 E. 69th Street, Suite 108, New York, New York 10021, Telephone: 6469626192, Fax: 6469620129, jkm2001@med.cornell.edu.

Disclosures/Conflicts: The funder of the study had no role in study design, data collection, data analysis, data interpretation, or writing of the report. The corresponding author had full access to all the data in the study and had final responsibility for the decision to submit for publication. Dr. Chang receives funding from by Leading Foreign Research Institute Recruitment Program through the National Research Foundation of Korea funded by the Ministry of Science and ICT (Grant No. 2012027176); Dr. Min receives funding from the National Institutes of Health (Grant Nos. R01 HL111141, R01 HL115150, R01 118019, and U01 HL 105907), the Qatar National Priorities Research Program (Grant No. 09-370-3-089), and GE Healthcare. Dr. Min served as a consultant to HeartFlow, serves on the scientific advisory board of Arineta, and has an equity interest in MDDX. Dr. Bax receives unrestricted research grants from Biotronik, Medtronic, Boston Scientific and Edwards Lifesciences. Dr. Leipsic serves as a consultant and has stock options in HeartFlow and Circle Cardiovascular Imaging, and receives speaking fees from GE Healthcare. Dr. Budoff receives grant support from the National Institutes of Health and General Electric. Dr. Samady receives grant support from Phillips/Volcano and St. Jude Abbott/Medtronic/Gilead. Dr. Chow holds the Saul and Edna Goldfarb Chair in Cardiac Imaging Research and receives research support from CV Diagnostix and educational support from TeraRecon Inc. Dr. Pontone receives institutional research grants from GE Healthcare, HeartFlow, Medtronic, Bracco, and Bayer. Dr. Virmani has received institutional research support from 480 Biomedical, Abbott Vascular, ART, BioSensors International, Biotronik, Boston Scientific, Celonova, Claret Medical, Cook Medical, Cordis, Edwards Lifescience, Medtronic, MicroVention, OrbusNeich, ReCord, SINO Medical Technology, Spectranetics, Surmodics, Terumo Corporation, W.L. Gore and Xeltis. Dr. Virmani also receives honoraria from 480 Biomedical, Abbott Vascular, Boston Scientific, Cook Medical, Lutonix, Medtronic, Terumo Corporation, and W.L. Gore, and is a consultant for 480 Biomedical, Abbott Vascular, Medtronic, and W.L. Gore. All other authors have no conflicts of interest to disclose.

Imaging Center, SDN IRCCS, Naples, Italy [6]Department of Cardiology, William Beaumont Hospital, Royal Oak, Michigan [7]Department of Medicine and Radiology, University of Ottawa, Ontario, Canada [8]Department of Radiology, Miami Cardiac and Vascular Institute, Miami, FL [9]Department of Radiology, Medical University of Innsbruck, Innsbruck, Austria [10]Department of Radiology and Nuclear Medicine, German Heart Center Munich, Munich, Germany [11]Seoul National University College of Medicine, Seoul National University Hospital, Seoul, South Korea [12]Department of Medicine and Radiology, University of British Columbia, Vancouver, British Columbia, Canada [13]Department of Radiology, Area Vasta 1/ASUR Marche, Urbino, Italy [14]UNICA, Unit of Cardiovascular Imaging, Hospital da Luz, Lisboa, Portugal [15]Cardiology Service, Walter Reed National Military Center, Bethesda, Maryland [16]Chung-Ang University Hospital, Seoul, South Korea [17]VU University Medical Center, Amsterdam, the Netherlands [18]Asan Medical Center, University of Ulsan College of Medicine, Seoul, South Korea [19]Department of Radiology, Mayo Clinic, Rochester, Minnesota [20]Department of Imaging and Medicine, Cedars Sinai Medical Center, Los Angeles, California [21]Department of Medicine, Los Angeles Biomedical Research Institute, Torrance, CA [22]Division of Cardiology, Emory University School of Medicine, Atlanta, Georgia [23]Division of Cardiovascular Medicine, Brigham and Women's Hospital, Boston, Massachusetts [24]CVPath Institute, Gaithersburg, Maryland [25]Icahn School of Medicine at Mount Sinai, Mount Sinai Heart, Zena and Michael A. Wiener Cardiovascular Institute, and Marie-Josée and Henry R. Kravis Center for Cardiovascular Health, New York, New York

Abstract

Background—The association of atherosclerotic features with first acute coronary syndromes (ACS) has not accounted for plaque burden.

Objectives—To identify atherosclerotic features associated with precursors of ACS.

Methods—We performed a nested case:control study within a cohort of 25,251 patients undergoing coronary computed tomographic angiography (CCTA) with follow-up over 3.4±2.1 years. ACS patients and non-events with no prior coronary artery disease (CAD) were propensity matched 1:1 for risk factors and CCTA-evaluated obstructive (≥50%) CAD. Separate core labs performed blinded adjudication of ACS and culprit lesions and quantification of baseline CCTA for % diameter stenosis (%DS), % cross-sectional plaque burden (PB), plaque volumes (PV) by composition (calcified, fibrous, fibro-fatty, and necrotic core), and presence of high-risk plaques (HRP).

Results—We identified 234 ACS and control pairs (62 years, 63% male). Over 65% of ACS patients had non-obstructive CAD at baseline, and 52% had HRP. %DS, cross-sectional PB, fibro-fatty and necrotic core volume, and HRP increased the adjusted hazard ratio (HR) of ACS [1.010 per %DS, 95% confidence interval (CI) 1.005–1.015; 1.008 per % cross-sectional PB, 95% CI 1.003–1.013; 1.002 per mm^3 fibro-fatty plaque, 95% CI 1.000–1.003; 1.593 per mm^3 necrotic core, 95%CI 1.219–2.082; all p <0.05]. Of the 129 culprit lesion precursors identified by CCTA, three-fourths exhibited <50% stenosis and 31.0% exhibited HRP.

Conclusion—Although ACS increases with %DS, most precursors of ACS cases and culprit lesions are non-obstructive. Plaque evaluation, including HRP, PB, and plaque composition, identifies high risk patients above and beyond stenosis severity and aggregate plaque burden.

Keywords

Coronary artery disease; acute coronary syndrome; coronary computed tomography angiography; atherosclerosis; clinical outcome

Introduction

Prior invasive and pathologic studies have identified coronary atherosclerotic plaque features that are central to the pathogenesis of acute coronary syndromes (ACS) (1,2). These include measures of coronary luminal narrowing, plaque burden, arterial remodeling, and plaque composition including thin cap fibroatheroma, necrotic core and spotty calcification (2–6). However, these findings have been largely derived from atherosclerotic evaluation simultaneous or subsequent to ACS, to partial samples of the coronary artery tree, and to secondary prevention populations (3–5). The utility of vulnerable plaque evaluation in comparison to overall atherosclerotic disease burden has been debated, especially given the technical difficulty of invasive plaque characterization (7).

Coronary computed tomography angiography (CCTA) is a non-invasive test that enables evaluation of all coronary arteries and their branches in patients with suspected or known coronary artery disease (CAD). The high accuracy of CCTA for detection and exclusion of CAD is well reported, and recent advances in CT technologies now allow for coronary atherosclerotic quantification and characterization with high diagnostic performance when compared to invasive reference standards (8,9). Limited studies have employed CCTA to identify atherosclerotic plaque features associated with ACS (9,10). To date, these studies have used non-standardized image analysis protocols, non-quantitative methods, mixed populations of patients with and without known CAD, smaller and largely single-center studies, and cohorts with few events (4,9–11).

As CCTA is routinely performed in those with suspected but without manifest CAD, it offers a unique opportunity to describe the natural history of atherosclerosis in a primary prevention population of stable patients before ACS occurrence, whilst accounting for the totality of atherosclerotic features in all coronary arteries and their branches at the patient level (11,12). We aimed to elucidate the prognostic significance of coronary atherosclerosis plaque features for identification of stable patients who will experience future ACS from a nested case:control study within a large international multicenter cohort of 25,251 consecutive patients without known CAD undergoing CCTA (13).

Methods

Study Design and Study Population

The ICONIC (Incident COroNary Syndromes Identified by Computed Tomography) study is a nested case:control study of patients without known CAD within the dynamic CONFIRM registry, a longitudinal observational cohort study of consecutive individuals undergoing

CCTA (13). From this registry, 13 sites from eight countries (the United States, Canada, Germany, Austria, Italy, the Netherlands, Portugal, and South Korea) collected consecutive patients with baseline CCTA for a total of 25,416 patients with follow-up for 99.6% over 3.4 ± 2.1 years for all-cause mortality and 95.4% over 3.4 ± 2.1 years for MACE events (Figure 1, Online Appendix I). Physicians or nurses at each site prospectively collected CAD history and risk factors, and symptoms at the time of baseline CCTA, coded CCTA stenosis severity by segment then collected site adjudication of ACS and death. In the present study, patients were eligible if they had had no prior CAD, as defined by no prior revascularization or myocardial infarction, and baseline CCTA with follow-up of ACS. Patients with deaths without antecedent ACS were censored (Figure 1, Online Appendix II). Candidate patients experiencing site-adjudicated ACS were matched 1:1 to within-site controls who did not experience ACS. Sites submitted supporting data for ACS, as well as baseline CCTA images, for cases and controls. Each site obtained local institutional review board or ethics board approval and submitted study ID-coded data stripped of protected health information for central adjudication and CCTA measurement.

The Clinical and Data Coordinating Center (CDCC) at the Dalio Institute of Cardiovascular Imaging performed uniform adjudication of ACS masked to CCTA evaluation using definitions set forth by the World Health Organization (WHO) (14). The CCTA Core Laboratory (CCTA-CL) at Severance Hospital of Yonsei University performed comprehensive and quantitative analysis of CCTAs blinded to case status. The final study population consisted of CDCC-adjudicated ACS and their paired within-site controls that had CCTA-CL measured baseline CCTA.

Among 25,251 patients with follow-up for MACE events (804 site-reported ACS, 3.2%) at 13 sites over 3.4 ± 2.1 years, 2451 patients (221 site-reported ACS) were excluded for prior CAD or death without ACS, leaving 22,800 (583 site-reported ACS) eligible for the study. After exclusion of site-reported ACS with insufficient or absent clinical data (n=181), with ACS in an interval revascularized coronary segment (n=29), with adjudication by the CDCC as not meeting criteria for ACS (n=19), without CCTA data to submit to the CL (n=95), or with CCTA data that was not interpretable for CL measurements (n=25), the final ICONIC study cohort comprised of 234 ACS cases and 234 propensity-matched controls (Figure 1).

Propensity Score Matching

Matching factors were determined *a priori* and all variables forced into propensity scoring using logistic regression were used to predict ACS in the main model. Factors entered into propensity scoring procedures included age, male sex, hypertension, hyperlipidemia, diabetes mellitus, family history of premature CAD, current smoking, and CAD severity assessed by CCTA, defined as non-obstructive, one-vessel, two-vessel, or three-vessel/left main disease at the 50% diameter stenosis threshold (area under the receiver-operating curve 0.94, 95% confidence interval (CI) 0.92–0.95, Online Appendix III). A nearest-neighbor approach using 1:1 matching was performed on site and propensity score with a greedy matching technique to match all cases. Relaxed models for missing variables were utilized to allow all cases to be matched regardless of missing data (15).

ACS Event Adjudication

The CDCC reviewed ACS event data including cardiac enzyme measurement, electrocardiograms and invasive coronary angiograms (ICA) blinded to CCTA data; and adjudicated ACS using the WHO/MONICA universal definition of myocardial infarction (Online Appendix IV) (14,16). For ACS cases that underwent ICA at the time of ACS, one culprit lesion per patient was adjudicated blinded to CCTA data using the modified ROMICAT definition and coded using a modified Society of Cardiovascular Computed Tomography (SCCT) 18-segment coronary tree (Online Appendix V) (11). ACS cases with culprit lesions in interval revascularized segments were excluded.

Among 234 patients with adjudicated ACS, 32 patients were excluded for absence of ICA performance, 26 patients were excluded for unavailable ICA to adjudicate a culprit lesion, and 14 patients underwent ICA with no culprit lesion that could be determined, leaving 162 patients with adjudicated culprit lesions. The 72 ACS cases without adjudicated culprits did not differ from the 162 cases with adjudicated culprits in age, sex, and type of ACS but did exhibit fewer lesions and lesser %DS (Online Appendix, Table VII-4).

Baseline CCTA Analysis

Baseline CCTA performance and site interpretation was performed using CT scanners of ≥64-detector rows in direct accordance with SCCT guidelines (12,17). The CCTA-CL analyzed site-submitted DICOM files masked to clinical results and case status. Independent level III-experienced readers at the CCTA-CL performed standardized measurements using semiautomated plaque analysis software (QAngioCT Research Edition v2.1.9.1; Medis Medical Imaging Systems, Leiden, the Netherlands (Central Illustration) with appropriate manual correction (18).

Briefly, for each segment of the 18-segment SCCT model with a diameter ≥2 mm (Online Appendix VI), quantitative analysis was performed on every 1-mm cross-section to measure vessel length, volume, plaque volume (PV), mean plaque burden (PB), and plaque composition using predefined Hounsfield units (HU) thresholds: necrotic core (−30 to 30), fibro-fatty (30–130), fibrous (131–350) and calcified plaque (≥350) (12,19). The interobserver and intraobserver intraclass correlation for total plaque volume was 0.992 and 0.996 ($p<0.001$ respectively). The interobserver and intraobserver intraclass correlation for plaque composition ranged from 0.95–0.99 (Online Appendix, Table VI-1).

Additionally, for each lesion, measurements were performed of length, volume and plaque composition, as well as percent diameter stenosis (%DS), area stenosis, minimum luminal diameter, minimum luminal area, cross-sectional PB, mean PB, and remodeling index (Online Appendix VI) (20). Cutpoints of ≥50% and ≥70% %DS were used for obstructive CAD. Binary evaluation of adverse plaque characteristics included positive remodeling (PR), low attenuation plaque (LAP), spotty calcification (SC), bifurcation, and tortuosity. High-risk plaque (HRP) was defined as the presence within a coronary lesion of ≥2 features including PR, LAP, or SC (9,10). Segment-based plaque volumes and lesion-based measurements were summarized to the patient level, and diffuseness of atherosclerosis calculated as the ratio of summed lesion lengths and total vessel length.

Subsequent to CCTA-CL analysis, ICA-identified culprit lesions were co-registered to the baseline CCTA precursor lesions (D.H. and F.Y.L.) by comparison of coronary segment coding and using distance from ostia and coronary vessel branch points as fiduciary landmarks. Unblinded comparison of ICA and CCTA was allowed for alignment of lesions but not for reclassification of ACS.

Statistical Analysis

At the patient level, ACS patients were compared 1:1 to matched patients who did not experience ACS. At the lesion level, culprit lesion precursors were compared: 1) within-subject, to all remaining non-culprit lesions in the same ACS patient; 2) within-subject, to the non-culprit lesion with the highest %DS in the same ACS patient; and 3) between-subject, to the lesion with the highest %DS in the paired control non-ACS patient.

Continuous variables are expressed as means ± standard deviation, and categorical variables are presented as absolute counts and percentages. Differences between categorical variables were analyzed using McNemar's test or chi-square test, as appropriate, and those between continuous variables using paired Wilcoxon Rank-sum.

Multivariate marginal Cox models adjusting for conventional clinical risk factors were employed to compare atherosclerotic plaque differences accounting for propensity matching between cases and controls (21). The robust variance estimator accounts for the clustering within matched pairs. For per-lesion level analysis, marginal Cox regression was used to account for patient effects (22,23). Components of the propensity score were not candidates for multivariate regression.

A p value <0·05 was considered to indicate a statistically significant difference. All analyses were performed with SAS (version 9.4, SAS Institute Inc., Cary, NC, USA) and R 3.3.0 (R Development Core Team, 2016).

Results

Baseline Patient Characteristics and Clinical Events

The final ICONIC study cohort comprised of 234 CDCC-adjudicated ACS cases and 234 propensity-matched controls with CCTA-CL measured baseline CCTA. The average age of the nested case:control cohort was 62.2 ± 11.5 years (63% male) with follow-up time of 3.9 ± 2.5 years. ACS and control patients were well matched by propensity score (0.07 ± 0.04 vs. 0.07 ± 0.04, p=0.73). ACS cases had lower rates of diabetes mellitus, a component of the propensity score (19.7% vs. 31.6%; p<0.001), and greater angina severity (p = 0.004, Online Appendix VII). Otherwise, there were no differences in baseline clinical risk factors, medications and lipid profiles.

ACS events comprised of 40 ST-elevation myocardial infarctions (STEMI), 114 non-STEMIs, 6 MIs wherein STEMI and NSTEMI could not be distinguished due to the timing of electrocardiogram relative to the ACS, and 74 cases of unstable angina pectoris. Culprit lesion precursors were identified by both ICA and baseline CCTA in 129 (53.4%) patients. During follow-up, ACS patients more frequently experienced interval revascularization

between baseline CCTA and last follow-up than controls (50.4% vs. 23.5%, p < 0.001), and the time to interval revascularization was shorter in cases, with a median of 26 (interquartile range 5,312) days compared to 64 (19, 199, p = 0.03) days.

Per-Patient Baseline CCTA Findings in ACS Patients and Controls

Overall, there were an average of 3.9 ± 2.5 lesions in ACS patients and 3.7 ± 2.7 lesions in controls (p = 0.40) (Table 1). The maximal %DS at the per-patient level was <50% for both ACS patients and controls (44.2 ± 26.4% vs. 33.7 ± 22.0%, p<0.001), with cases and controls exhibiting >50% stenosis in 34.6% vs. 19.2% and >70% stenosis in 12.8% vs. 5.1% respectively.

ACS patients did not differ significantly from controls by total plaque volume (289.7 ± 308.4 vs. 267.2 ± 285.7 mm^3, p = 0.321), calcified (97.7 ± 136.1 vs. 109.3 ± 164.0 mm3, p =0.389), or fibrous plaque volumes (126.8 ± 131.6 vs. 41.4 ± 62.2 mm^3, p = 0.137), but had significantly higher fibro-fatty (58.7 ± 85.8 vs. 41.4 ± 62.2 mm^3, p = 0.009) and necrotic core volumes (6.5 ± 14.0 vs. 4.2 ± 8.8 mm^3, p = 0.026). These findings remained consistent when plaque volumes were normalized to vessel volume. The maximal cross-sectional plaque burden was also significantly higher in cases than controls (66.1±25.8 vs. 56.5±28.7, p<0.001), with no significant difference in the mean plaque burden.

ACS patients exhibited HRP more frequently than controls (52.1% vs. 33.3%, p = 0.003) in addition to each component of HRP, including LAP, PR, and SC (all p < 0.05). ACS patients exhibited greater atherosclerotic plaque diffuseness, but did not differ from controls in atherosclerotic plaques at sites of vessel bifurcation or at tortuous points within the vessel (all p>0.05).

Per-Patient Baseline Atherosclerotic Plaque Precursors of ACS Events

In marginal Cox regression analysis adjusting for angina severity and interval revascularization, highest %DS severity was an indicator of future adverse event (HR 1.010 for every 1% increase in stenosis, 95% CI 1.005 to 1.015, p = 0.002), as well as the presence of high-grade coronary stenosis ≥70% (HR 1.536, 95% CI 1.141–2.067, p = 0.005, Table 2).

At the patient level, neither total plaque volume nor mean plaque burden was associated with an increased hazard of ACS occurrence (all p>0.05). However, fibro-fatty, necrotic core plaque and the sum of both were significant predictors for ACS (For every 1 mm^3 increase respectively, HR 1.002, 95% CI 1.000 – 1.004, p = 0.048; HR 1.013, 95% CI 1.003 – 1.022, p = 0.009; and HR 1.002, 95% CI 1.000 –1.003, p = 0.037). Calcified and fibrous plaque volumes were not associated with ACS (all p>0.05). The maximal cross-sectional plaque burden was also significantly associated with ACS (HR 1.008 for every %, 95% CI 1.003 – 1.013, p = 0.003).

The presence of HRP was associated with ACS (HR 1.593, 95% CI 1.219 – 2.082; p = 0.001), as were its constituents LAP (HR 1.378, 95% CI 1.051 – 1.805, p = 0.020) and SC (HR 1.543, 95% CI 1.169 – 2.037; p = 0.002). PR trended toward association with ACS (p=0.085).

Per-Lesion Baseline Atherosclerotic Plaque Precursors of ACS Culprit Lesions

Of the 162 patients with ICA available for culprit lesion adjudication, there were 129 cases where the culprit lesion by ICA could be aligned to a baseline lesion by CCTA with lesion measurements. The duration of time between baseline CCTA and follow-up ICA was median (IQR) of 0.08 (0.008, 1.42) years. In 21 cases, the culprit lesion aligned to normal segments on the baseline CCTA with no lesion measurements, and in the remaining 12 patients, the baseline lesion by CCTA could not be measured due to artifact or small vessel size. Over three-quarters of the 129 culprit lesion precursors exhibited <50% stenosis in the baseline CCTA (38.27 ± 20.97%), with relatively long lesions (35.90 ± 21.66 mm, Table 3). Overall plaque volume was 134.4 ± 141.5 mm^3, which was comprised of 44.88 ± 60.29 mm^3, 58.22 ± 62.39 mm^3, 28.47 ± 50.18 mm^3, and 2.85 ± 9.27 mm^3 of calcified, fibrous, fibro-fatty, and necrotic core volume, respectively (Central Illustration). The cross-sectional plaque burden was elevated (62.54±22.38). HRP was observed in 31.01% of culprit lesion precursors, and 24.03%, 76.74%, and 17.83% of culprit lesion precursors possessed LAP, PR, and SC, respectively.

Compared to within-subject non-culprit lesions, culprit-lesion precursors exhibited elevated hazard for greater %DS (HR 1.023 per % increase, 95% CI 1.015–1.031, p <0.001), lesion length (HR 1.021 per mm of length, 95% CI 1.013–1.029, p < 0.001), plaque volume (1.002 per mm^3 of volume, 95% CI 1.001–1.003, p<0.001) and all plaque constituents (p < 0.001 for all), notably fibro-fatty and necrotic core volume (1.007 per mm^3, 95% CI 1.003–1.010, p < 0.001). Culprit lesions also exhibited elevated hazard for cross-sectional plaque burden (1.027 per % increase, 95% CI 1.018–1.035, p<0.001), HRP (1.954, 95% CI 1.317–2.899, p = 0.001), LAP (1.805, 95% CI 1.198–2.721, p = 0.005), and SC (1.702, 95% CI 1.064–2.722, p = 0.026). Comparison to between-subject control lesions with highest %DS and to within-subject non-culprits with highest %DS demonstrated a consistent attenuation of the association with %DS, calcified PV and fibrous PV (p>0.05 for all). Total plaque volume, mean plaque burden, fibro-fatty and necrotic core volume, and HRP exhibited elevated hazards with variable statistical significance depending upon the choice of control.

Discussion

In this nested case-control study from a large prospective multinational registry of patients undergoing CCTA, we observed measures of coronary luminal narrowing to be associated with but generally imprecise discriminators of future ACS. At the patient level, only 34.6% possessed a coronary lesion with ≥50% diameter stenosis prior to ACS, with only 12.8% exhibiting ≥70% stenosis. These findings were further accentuated at the lesion level wherein precursor lesions of culprit plaques were identified as causing ≥50% and ≥70% luminal obstruction only 24.8% and 4.7% of the time, respectively.

One major limitation of the extant literature on vulnerable plaque characterization is that its predictive value has not accounted for the denominator of atherosclerotic disease burden in the vulnerable patient (7,24). Our study fills an important knowledge gap as case and control patients were propensity matched for major patient-level characteristics including clinical risk factors and number of obstructive coronary vessels, and did not differ by total plaque volume or mean plaque burden. We observed that lesion morphology, inclusive of cross-

sectional plaque burden, HRP, LAP, PR and SC, and plaque burden by composition, had independent predictive value for ACS, above and beyond clinical risk factors and total atherosclerotic disease burden.

Our per-lesion level results underline the complementary importance of atherosclerotic disease burden in relation to plaque morphology and composition. In unmatched analyses, culprit lesion precursors compared to other lesions within case patients displayed increased plaque volume, greater length, as well as greater %DS, cross-sectional plaque burden, composition-specific plaque volumes, and prevalence of HRP. When compared to between-patient control lesions or within-patient non-culprit lesions with the highest luminal narrowing, the association with calcified and fibrous plaque volumes was weakened. Thus, atherosclerotic plaque burden is an important marker of lesions at risk, but controlling for plaque burden there is independent prognostic value of plaque features and composition. Additionally, within a single patient or compared to a control, future culprit lesions share many common features with baseline stenotic lesions, but the presence of lesions with high risk plaque features and fibrofatty or necrotic core demarcate risk on a per-lesion and per-patient level.

Our results confirm the findings of prior landmark studies using invasive coronary angiography, demonstrating that although %DS is a strong indicator of future adverse events, only a minority of ACS culprit lesion precursors cause significant coronary artery luminal narrowing prior to ACS occurrence, even with a shorter duration between baseline CCTA and ICA (25,26). Our results additionally confirm the association of ACS with findings posited by pathologic and invasive imaging studies, including plaque volumes, necrotic and fibro-fatty plaque compositions, and HRP features (3,5). In the PROSPECT study, the sole multicenter prospective study of vulnerable plaque characteristics to date, among patients undergoing a repeat PCI in nearly all cases for increasing angina as their clinical presentation, the baseline intravascular ultrasound predictors of future ACS included minimum luminal area, cross-sectional plaque burden, and thin cap fibroatheroma (5,27). Our study found congruent results with %DS, cross-sectional plaque burden, and HRP findings associated with thin cap fibroatheroma including LAP (28). Our study findings extend the scope of these pathologic and invasive studies to a primary prevention population, with ACS rather than angina outcomes, and using a matched case:control population wherein differences in coronary luminal and atherosclerotic plaque features would be expectedly causal to the event (5,27). Finally, in the largest international multicenter cohort of ACS patients, our results demonstrate the prognostic value and generalizability of noninvasive plaque evaluation across a broad array of countries, CCTA scanners and protocols, and strengthens prior observations with invasive studies in that the majority of our outcome events were myocardial infarctions, and not unstable or increasing angina.

Prior CCTA studies have similarly evaluated the importance of atherosclerotic plaque features for prognosticating ACS. Limited to single centers, these studies have nevertheless highlighted the benefit of morphologic coronary assessment of LAP, PR and SC(4,9,10). Our study extends these pioneering studies by demonstrating the predictive value of noninvasive plaque quantitation by composition as well as morphology. We also highlight the

significance of cross-sectional plaque burden in CCTA evaluation, which has previously been emphasized only in the invasive imaging literature.

Our observation of gradations of risk within categories of non-calcified plaque, most notably for fibro-fatty and necrotic volumes, integrates the literature correlating CCTA plaque composition to pathology and invasive imaging. Current generation CCTA lacks the spatial resolution to visualize fibrous cap thickness to characterize thin cap fibroatheroma; hence, CCTA plaque evaluation must rely on methods that focus on luminal, vessel remodeling, and plaque composition using HU thresholds, such as HU<30, that are associated with necrotic core, and morphologic HRP criteria such as LAP, SC and PR that are associated with thin cap fibroatheroma (28,29). Thresholds for calcium, necrotic core, and intermediate degrees of fibrous tissue have largely been validated against virtual histology-intravascular ultrasound (VH-IVUS), but against the gold standard of histopathology, the HU of necrotic core and fibrous plaque demonstrates significant overlap (19,30). Conversely, the low risk of calcified plaque is consistent with VH-IVUS studies demonstrating that transformation of non-calcified plaques to calcified plaques is associated with a more benign prognosis (31). The implication for CCTA patient evaluation is that there is a continuum of risk by plaque composition, with greater weight for lower attenuation plaque burden than calcified or higher attenuation noncalcified plaque.

Taken together, the aforementioned findings allow several conclusions to be drawn at both the lesion and patient level. First, coronary luminal narrowing is a prognostic indicator of future ACS, but a threshold of ≥50% has low sensitivity for patients and lesions that will result in ACS, highlighting the need for additional or improved markers of risk. Furthermore, the present data support that within a patient, it is the lesion with greatest overall PV as well as fibro-fatty and necrotic core PV that has the greatest probability of becoming a culprit ACS lesions, but not necessarily the one displaying the highest %DS. From the results of this study, when aiming to discriminate a patient as having risk or no risk of ACS, it appears essential to integrate atherosclerosis feature findings with consideration of PV and presence of HRPs. Second, consistent with the dynamic nature of HRP and the frequent observation of clinically silent healed ruptures, we observed a relatively low sensitivity of HRP of 69% to predict a culprit lesion on a per-lesion basis, with a higher sensitivity on a per-patient basis. We posit that atherosclerotic plaque features represent a dimension of disease burden that may better identify at-risk patients on a whole patient basis. That is, individual plaque imaging may signal more information about the patient than about the individual lesion or the total plaque burden alone. Finally, we observed that in 21 of the 162 patients with ICA available, the culprit lesion aligned to normal segments on the baseline CCTA. This may represent baseline non-obstructive plaque below the spatial resolution of CCTA, interval rapid plaque progression, or mechanisms of acute coronary events other than plaque rupture, such as plaque erosion. Our study design did not prescribe repeat CCTA, but prospective studies with serial CCTA are needed to address plaque progression in previously normal segments.

Our study is not without limitations. First, derived from a large observational cohort study, these present findings are susceptible to unmeasured confounding factors, and referral bias and potential biases in propensity matched controls. Indications for CCTA were for

evaluation of CAD in clinically stable patients, as the CONFIRM registry included many patients from non-US sites and with CCTAs prior to the introduction of appropriate use criteria. However, use of the existing cohort study allowed collection of the largest international multicenter cohort of atherosclerotic plaque precursors to ACS to date. Second, to ensure proper adjudication of ACS events, we censored patients who died without confirmatory findings of ACS. Thus, these findings should be considered limited to patients at risk of experiencing non-fatal ACS and future studies should now be performed to determine whether the present findings apply to fatal ACS. Missing adjudication data may also contribute to information bias. Third, propensity score matching on the likelihood of ACS results in well-matched controls with complete and careful CCTA measurements but reduces generalizability to the general pool of patients undergoing CCTA (Online Appendix VIII). Prediction models will require prospective cohorts in a generally low-risk population and, given the time and costs of quantitative CT, may be economically feasible only with completely automated CCTA measurements or deep learning. Fourth, atherosclerotic quantification and characterization was performed only on a single baseline CCTA. Thus, information related to atherosclerosis progression or transformation as related to time to ACS occurrence remains unknown.

Conclusions

Despite advances in risk stratification, acute coronary syndromes remain burdensome and unpredictable, and an integrated evaluation of vulnerable plaque identifies the vulnerable patient above and beyond the clinical risk factors and aggregate plaque burden. In this multicenter case-control study of stable patients without known CAD, the majority did not possess high-grade coronary stenosis before experiencing ACS. Coronary atherosclerotic precursors of ACS exhibited elevated fibro-fatty and necrotic core volumes, but not total or calcified volumes. HRP and its features of LAP, PR, and SCs, as well as cross-sectional plaque burden, also identify lesions and patients that will experience ACS. Both on a per-plaque as well as per-patient basis, perhaps of greatest import is the finding of the robust incremental prognostic information when accounting for the atherosclerotic plaque features that contribute to a coronary stenosis rather than just the stenosis itself. Our data suggest a potential paradigm shift wherein targeted treatment of patients and lesions possessing high-risk atherosclerotic plaque characteristics may improve therapeutic precision and outcomes. Future studies addressing this approach now appear warranted.

Acknowledgments

Funding: This trial was supported by NIH Grant No HL115150 and the Leading Foreign Research Institute Recruitment Program of the National Research Foundation of Korea, Ministry of Science, ICT & Future Planning (Seoul, Korea).

Abbreviations

CAD	Coronary artery disease
CCTA	Coronary computed tomography angiography
CDCC	Clinical and Data Coordinating Center

CI	Confidence interval
DS	Diameter Stenosis
FF	Fibro-fatty
HRP	High-risk plaque
HU	Hounsfield Unity
ICA	Invasive coronary angiography
IVUS	Intravascular ultrasound
LAP	Low-attenuation plaque
MACE	Major adverse cardiac events
NC	Necrotic core
NSTEMI	Non-ST-elevation myocardial infarction
PB	Plaque burden
PR	Positive remodeling
PV	Plaque volume
SC	Spotty calcification
STEMI	ST-elevation myocardial infarction

References

1. Schoenhagen P, Ziada KM, Kapadia SR, Crowe TD, Nissen SE, Tuzcu EM. Extent and direction of arterial remodeling in stable versus unstable coronary syndromes. Circulation. 2000; 101:598–603. [PubMed: 10673250]
2. Virmani R, Burke AP, Farb A, Kolodgie FD. Pathology of the vulnerable plaque. J Am Coll Cardiol. 2006; 47:C13–C18. [PubMed: 16631505]
3. Yamagishi M, Terashima M, Awano K, et al. Morphology of vulnerable coronary plaque: insights from follow-up of patients examined by intravascular ultrasound before an acute coronary syndrome. J Am Coll Cardiol. 2000; 35:106–111. [PubMed: 10636267]
4. Motoyama S, Sarai M, Harigaya H, et al. Computed tomographic angiography characteristics of atherosclerotic plaques subsequently resulting in acute coronary syndrome. J Am Coll Cardiol. 2009; 54:49–57. [PubMed: 19555840]
5. Stone GW, Maehara A, Lansky AJ, et al. A prospective natural-history study of coronary atherosclerosis. N Engl J Med. 2011; 364:226–235. [PubMed: 21247313]
6. Ehara S, Kobayashi Y, Yoshiyama M, et al. Spotty calcification typifies the culprit plaque in patients with acute myocardial infarction: an intravascular ultrasound study. Circulation. 2004; 110:3424–9. [PubMed: 15557374]
7. Arbab-Zadeh A, Fuster V. The myth of the “vulnerable plaque”: transitioning from a focus on individual lesions to atherosclerotic disease burden for coronary artery disease risk assessment. J Am Coll Cardiol. 2015; 65:846–855. [PubMed: 25601032]
8. Budoff MJ, Dowe D, Jollis JG, et al. Diagnostic performance of 64-multidetector row coronary computed tomographic angiography for evaluation of coronary artery stenosis in individuals without

known coronary artery disease: results from the prospective multicenter ACCURACY (Assessment by Coronary Computed Tomographic Angiography of Individuals Undergoing Invasive Coronary Angiography) trial. J Am Coll Cardiol. 2008; 52:1724–1732. [PubMed: 19007693]

9. Motoyama S, Ito H, Sarai M, et al. Plaque Characterization by Coronary Computed Tomography Angiography and the Likelihood of Acute Coronary Events in Mid-Term Follow-Up. J Am Coll Cardiol. 2015; 66:337–46. [PubMed: 26205589]
10. Puchner SB, Liu T, Mayrhofer T, et al. High-risk plaque detected on coronary CT angiography predicts acute coronary syndromes independent of significant stenosis in acute chest pain: results from the ROMICAT-II trial. J Am Coll Cardiol. 2014; 64:684–692. [PubMed: 25125300]
11. Hoffmann U, Moselewski F, Nieman K, et al. Noninvasive assessment of plaque morphology and composition in culprit and stable lesions in acute coronary syndrome and stable lesions in stable angina by multidetector computed tomography. J Am Coll Cardiol. 2006; 47:1655–1662. [PubMed: 16631006]
12. Leipsic J, Abbara S, Achenbach S, et al. SCCT guidelines for the interpretation and reporting of coronary CT angiography: a report of the Society of Cardiovascular Computed Tomography Guidelines Committee. J Cardiovasc Comput Tomogr. 2014; 8:342–358. [PubMed: 25301040]
13. Min JK, Dunning A, Lin FY, et al. Rationale and design of the CONFIRM (coronary CT angiography evaluation for clinical outcomes: an international multicenter) registry. J Cardiovasc Comput Tomogr. 2011; 5:84–92. [PubMed: 21477786]
14. Mendis S, Thygesen K, Kuulasmaa K, et al. World Health Organization definition of myocardial infarction: 2008–09 revision. Int J Epidemiol. 2011; 40:139–46. [PubMed: 20926369]
15. Austin PC. An introduction to propensity score methods for reducing the effects of confounding in observational studies. Multivariate behavioral research. 2011; 46:399–424. [PubMed: 21818162]
16. Thygesen K, Alpert JS, Jaffe AS, et al. Third universal definition of myocardial infarction. Eur Heart J. 2012; 33:2551–2567. [PubMed: 22922414]
17. Abbara S, Blanke P, Maroules CD, et al. SCCT guidelines for the performance and acquisition of coronary computed tomographic angiography: A report of the society of Cardiovascular Computed Tomography Guidelines Committee: Endorsed by the North American Society for Cardiovascular Imaging (NASCI). J Cardiovasc Comput Tomogr. 2016; 10:435–449. [PubMed: 27780758]
18. Park H-B, Lee BK, Shin S, et al. Clinical Feasibility of 3D Automated Coronary Atherosclerotic Plaque Quantification Algorithm on Coronary Computed Tomography Angiography: Comparison with Intravascular Ultrasound. European radiology. 2015:1–11.
19. de Graaf MA, Broersen A, Kitslaar PH, et al. Automatic quantification and characterization of coronary atherosclerosis with computed tomography coronary angiography: cross-correlation with intravascular ultrasound virtual histology. The international journal of cardiovascular imaging. 2013; 29:1177–1190. [PubMed: 23417447]
20. Fihn SD, Gardin JM, Abrams J, et al. 2012 ACCF/AHA/ACP/AATS/PCNA/SCAI/STS guideline for the diagnosis and management of patients with stable ischemic heart disease: a report of the American College of Cardiology Foundation/American Heart Association task force on practice guidelines, and the American College of Physicians, American Association for Thoracic Surgery, Preventive Cardiovascular Nurses Association, Society for Cardiovascular Angiography and Interventions, and Society of Thoracic Surgeons. J Am Coll Cardiol. 2012; 60:e44–e164. [PubMed: 23182125]
21. Austin PC. The use of propensity score methods with survival or time-to-event outcomes: reporting measures of effect similar to those used in randomized experiments. Statistics in Medicine. 2014; 33:1242–1258. [PubMed: 24122911]
22. Lin DY, Wei LJ. The Robust Inference for the Cox Proportional Hazards Model. Journal of the American Statistical Association. 1989; 84:1074–1078.
23. Wei LJ, Lin DY, Weissfeld L. Regression Analysis of Multivariate Incomplete Failure Time Data by Modeling Marginal Distributions. Journal of the American Statistical Association. 1989; 84:1065–1073.
24. Libby P, Pasterkamp G. Requiem for the ‘vulnerable plaque’. Eur Heart J. 2015:ehv349.
25. Maddox TM, Stanislawski MA, Grunwald GK, et al. Nonobstructive coronary artery disease and risk of myocardial infarction. JAMA. 2014; 312:1754–1763. [PubMed: 25369489]

26. Ambrose JA, Tannenbaum MA, Alexopoulos D, et al. Angiographic progression of coronary artery disease and the development of myocardial infarction. J Am Coll Cardiol. 1988; 12:56–62. [PubMed: 3379219]

27. Tian J, Ren X, Vergallo R, et al. Distinct morphological features of ruptured culprit plaque for acute coronary events compared to those with silent rupture and thin-cap fibroatheroma: a combined optical coherence tomography and intravascular ultrasound study. J Am Coll Cardiol. 2014; 63:2209–2216. [PubMed: 24632266]

28. Maurovich-Horvat P, Hoffmann U, Vorpahl M, Nakano M, Virmani R, Alkadhi H. The napkin-ring sign: CT signature of high-risk coronary plaques? JACC Cardiovascular imaging. 2010; 3:440–4. [PubMed: 20394906]

29. Nakazato R, Otake H, Konishi A, et al. Atherosclerotic plaque characterization by CT angiography for identification of high-risk coronary artery lesions: a comparison to optical coherence tomography. Eur Heart J Cardiovasc Imaging. 2015 Apr; 16(4):373–9. doi:10.1093/ehjci/jeu188. Epub 2014 Sep 21. [PubMed: 25246503]

30. Boogers MJ, Broersen A, van Velzen JE, et al. Automated quantification of coronary plaque with computed tomography: comparison with intravascular ultrasound using a dedicated registration algorithm for fusion-based quantification. Eur Heart J. 2012; 33:1007–16. [PubMed: 22285583]

31. Puri R, Nicholls SJ, Shao M, et al. Impact of statins on serial coronary calcification during atheroma progression and regression. J Am Coll Cardiol. 2015; 65:1273–1282. [PubMed: 25835438]

Appendix I. ICONIC study organization and list of participating sites and investigators

Executive committee: James K. Min, MD, Leslee J Shaw, MD, Renu Virmani, MD, Habib Samady, MD, Peter Stone, MD; Jagat Narula, MD; Fay Y. Lin, MD; Daniel Berman, MD; Matthew Budoff, MD

Clinical and Data Coordinating Center (CDCC): Subhi J. Al-Aref, MD; Iksung Cho, MD; Ibrahim Danad, MD; Aeshita Dwivedi, MD; Kimberly Elmore, MS; Donghee Han, MD; Ran Heo, MD; Ji-Hyun Lee, MD; Mahn-won Park, MD; Wijnand Stuijfzand, MD; Jessica Pena, MD; Asim Rivzi, MD; Hilary Soohoo, BA; Shenghao Chen, BA; Katie An, BA; Richard A Ferraro, MEd; Dan Gebow, PhD.

Data management and biostatistical analysis: Heidi Gransar, MSc; Yao Lu, MSc; Amit Kumar, MSc; Ji Min Sung, PhD

Clinical Events Adjudication Committee: Fay Y. Lin, MD; Lohendran Bhaskaran, MD, Iksung Cho, MD; Ibrahim Danad, MD; Donghee Han, MD; MD; Ji-Hyun Lee, MD; Joshua Schulman-Marcus, MD

CCTA Core Laboratory: Hyuk-Jae Chang, MD; Hyung-Bok Park, MD; Sang-Eun Lee, MD

Study sites, principal investigators, and primary study coordinators:

- Ottawa University of Ottawa Heart Institute: Benjamin Chow, MD; Owen Clarkin
- William Beaumont Hospital, City, Michigan, USA: Gilbert Raff, MD; Kavitha Chinnaiyan, MD; Ralph Gentry and Mark Pica

- Giovanni XXIII Hospital of Monastier/Academic Hospital of Parma: Filippo Cademartiri, MD PhD and Erica Maffei, MD
- German Heart Center Munich, Munich, Germany: Martin Hadamitzky, MD; Hanna Nieberler
- Severance Cardiovascular Hospital, Seoul, South Korea; Hyuk-Jae Chang, MD PhD; Sang-Eun Lee, MD
- Walter Reed Medical Center, Washington DC, USA: Todd Villines, MD
- Seoul National University Hospital, Seoul, South Korea: Yong-Jin Kim, MD PhD, Taekyeong Kim, MD.
- University of British Columbia, Vancouver, BC, Canada: Jonathon Leipsic, MD
- Innsbruck Medical University, Innsbruck, Austria: Gudrun Feuchtner, MD; Fabian Plank, MD; Harald G. Weirich, MD
- Baptist Hospital of Miami, Miami, Florida, USA: Ricardo Cury, MD; Cindy Stephens
- University of Milan, Centro Cardiologico Monzino, IRCCS Milan, Italy; Daniele Andreini, MD and Gianluca Pontone, MD; Edoardo Conte, MD
- UNICA, Hospital Da Luz, Lisbon, Portugal: Hugo Marques, MD
- Leiden University Medical Center, HARTZ, Leiden, the Netherlands: Jeroen Bax, MD PhD and Alexander van Rosendael, MD

Appendix II: Inclusion and exclusion criteria

- Inclusion criteria
  - 13 sites in North America, Europe and Asia
  - Baseline coronary computed tomographic angiography (CCTA) performed with prospective clinical data collection
  - Had follow-up for ACS events
- Exclusion Criteria
  - Cases and controls
    - Death before acute coronary syndrome (ACS)
    - Prior coronary artery disease (CAD)
    - CCTA images missing or uninterpretable for core lab quantitative CCTA measurement
  - Patient Cases
    - Insufficient data to adjudicate
    - Did not meet MONICA/WHO definition of ACS

- ♦ ACS occurred prior to CCTA
- ♦ Culprit lesion in segment with interval revascularization (percutaneous coronary intervention (PCI) or coronary artery bypass graft(CABG))

– Patient Controls

- ♦ Not propensity matched 1:1 to adjudicated case

Appendix III. Propensity scoring

Propensity score methods

The propensity score was derived from CONFIRM registry data of 15 sites that originally agreed to participate in ICONIC in 2012. Patients were eligible for the propensity score derivation cohort if they had follow-up for ACS events, and were either ACS events or nonevents. Patients with deaths were censored. Matching factors were determined a priori and all variables forced into propensity scoring using logistic regression were used to predict ACS in the main model. Factors entered into the score included age, gender, hypertension, hyperlipidemia, diabetes, family history, current smoking, and site-interpreted baseline CAD severity on CCTA categorized as nonobstructive<50%, single vessel obstructive, two vessel obstructive, and three vessel/left main obstructive >=50%. Relaxed propensity scores with variables dropped were additionally derived using the same cohort to allow assignment of a propensity score to all ACS in the presence of missing data. Balance of covariates was checked by deciles. Discrimination of the propensity score was evaluated with area under the receiver operating curve (AUC).

Propensity score results

The propensity score derivation patient population consisted of 24,600 patients with 861 ACS over 3.2 ± 1.9 years (Table 1--1). The full propensity score exhibited an area under the receiver-operating curve (AUC) of 0.94 (95% CI 0.92, 0.95, Figure III-1).

Table III-1

Full propensity score for likelihood of ACS

	Univariate		Multivariate	
Variable	**OR (95 CI)**	**P**	**OR (95 CI)**	**P**
Age	1.0 (1.0–1.1)	<0.001	1.0 (1.0–1.0)	<0.001
Male Gender	1.6 (1.4–1.8)	<0.001	1.1 (1.0–1.3)	0.12
HTN	1.7 (1.5–2.0)	<0.001	1.1 (0.9–1.3)	0.039
HL	1.3 (1.1–1.5)	<0.001	0.9 (0.7–1.0)	0.001
DM	2.0 (1.7–2.3)	<0.001	1.3 (1.1–1.6)	0.35
FH	1.1 (0.9–1.3)	0.23	1.1 (0.9–1.3)	0.23
Current TOB	1.2 (1.1–1.5)	0.009	1.2 (1.0–1.5)	0.023

	Univariate		Multivariate	
Variable	**OR (95 CI)**	**P**	**OR (95 CI)**	**P**
CAD Severity:				
Normal/Non-Obs	1.00		1.00	
1 VD	5.5 (4.6–6.5)	<0.001	4.6 (3.8–5.6)	<0.001
2 VD	6.6 (5.3–8.1)	<0.001	5.1 (4.1–6.4)	<0.001
3 VD/LM	9.5 (7.8–11.6)	<0.001	6.9 (5.5–8.6)	<0.001

HTN: hypertension. HL: hyperlipidemia. DM: diabetes. FH: family history. TOB: tobacco (smoking). VD: vessels diseased (obstructive ≥50%). LM: left main.

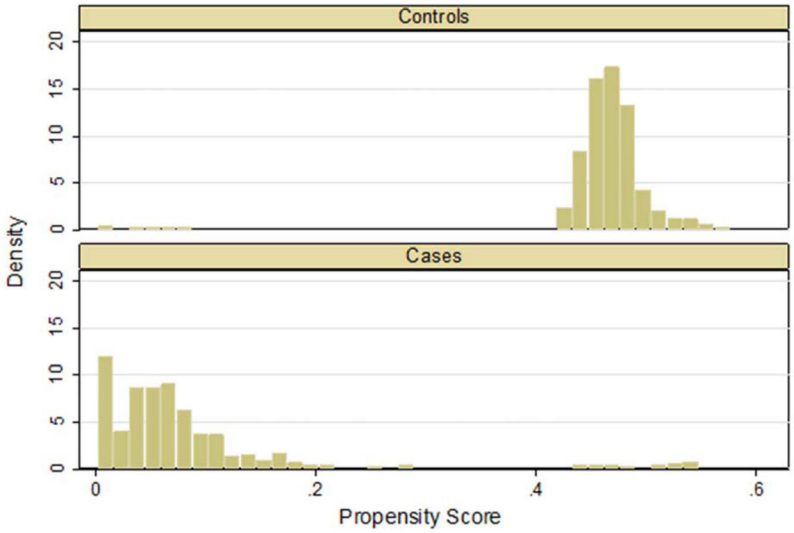

Figure III-1.
Propensity score distribution of candidate cases and controls prior to match

Propensity match methods

Site-adjudicated ACS cases were matched 1:1 with propensity-matched within-site controls from site-adjudicated nonevents stratified on site. Nearest-neighbor matching by propensity score was performed with a greedy matching technique to match all cases without replacement. A caliper width of 0.05 was used for matching.[1] Cases with missing CONFIRM data were matched to within-site controls using relaxed propensity scores, and the relaxed score was assigned as the summary propensity score. The same scores and technique were used to identify within-site controls for additional sites that subsequently joined the ICONIC study. Iterative rematching of within-site controls out of remaining unmatched non-events was performed when control CCTA DICOM images could not be obtained or control CCTA measurements could not be performed due to artifact, so that all centrally-adjudicated ACS would have matching propensity-matched controls with CCTA measurements. Finally, site-adjudicated ACS that did not meet criteria for centrally-adjudicated ACS or lacked CCTA measurements were excluded, as were their matched controls. With matching, the summary propensity score of AUC of candidate cases and

matched controls was 0.50 (95% CI 0.45, 0.55, Figure III-2). There was no significant difference between propensity scores in the CDCC-adjudicated cases and controls (0.07 ± 0.04 vs 0.07 ± 0.04, p = 0.73).

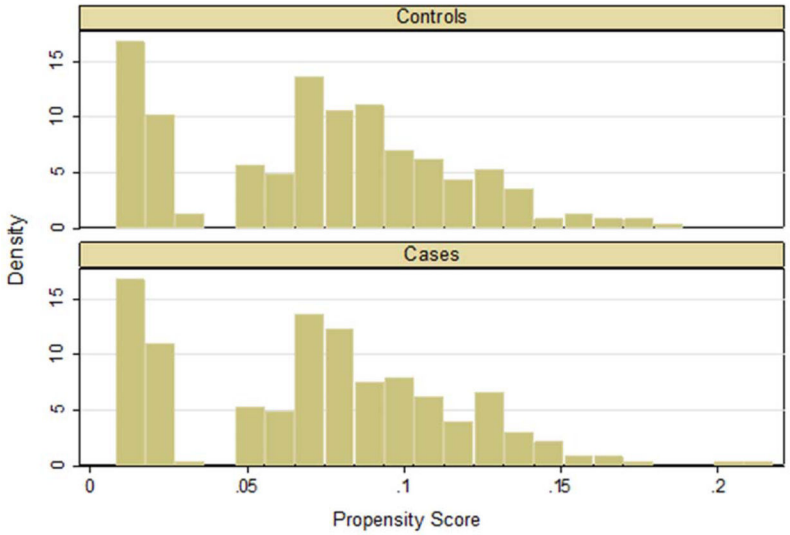

Figure III-2.
Propensity score distribution of the 234 case:control pairs in the ICONIC study

References

1. Austin PC. An Introduction to Propensity Score Methods for Reducing the Effects of Confounding in Observational Studies. Multivariate Behavioral Research. 2011; 46:399–424. [PubMed: 21818162]

Appendix IV. Event adjudication

Event adjudication was performed by six physicians (IC, LB, DH, JL, AR, FL) blinded to CCTA results, with two physician arbitrations of ambiguous cases. Symptoms of ischemia relied upon site report Cardiac enzyme, electrocardiogram (ECG), and invasive coronary angiography (ICA) data were used to adjudicate and classify candidate cases as ST-segment elevation myocardial infarction (STEMI), non-ST-segment elevation myocardial infarction (NSTEMI), or unstable angina (UA) using the WHO/MONICA third universal definition of myocardial infarction (MI).[1,2] Additionally, cases were adjudicated as unclassified MI in the presence of abnormal cardiac enzymes (>99% local upper limit of normal), the presence of other supporting information, and an ambiguous adjudication ECG unable to definitively classify STEMI/NSTEMI.

Cases that were adjudicated to be events other than STEMI, NSTEMI, unclassified MI or UA (i.e. myocarditis, Takotsubo cardiomyopathy, and congestive heart failure) were excluded. Cases that lacked cardiac enzyme data or had cardiac enzymes but insufficient clinical evidence of ischemia to determine adjudication were excluded.[3]

Additionally, all cases including MI and UA were classified by etiologic type modified from the third universal definition of MI as follows: 1) Type 1, Spontaneous ACS; 2) Type 2, ACS secondary to an ischemic imbalance; 3) Type 3 (ACS resulting in death when biomarkers were unavailable); (4) Type 4a (ACS related to PCI); (5) Type 4b (ACS related to stent thrombosis); and (6) Type 5 (ACS related to CABG), when culprit was in a bypass graft.[1] ACS of Types 4a, 4b and 5 were then excluded as events that could not be related to the lesions evaluated during baseline CCTA.

References

1. Thygesen K, Alpert JS, Jaffe AS, et al. Third universal definition of myocardial infarction. European heart journal. 2012; 33:2551–67. [PubMed: 22922414]
2. Mendis S, Thygesen K, Kuulasmaa K, et al. World Health Organization definition of myocardial infarction: 2008–09 revision. International journal of epidemiology. 2011; 40:139–46. [PubMed: 20926369]
3. Amsterdam EA, Wenger NK, Brindis RG, et al. AHA/ACC guideline for the management of patients with non-ST-elevation acute coronary syndromes. Circulation. 2014; 2014 CIR. 0000000000000134.

Appendix V. Culprit lesion precursor determination

ICA determination of culprit lesions

Sites performed ICA in accordance with typical clinical indications and imaging standards set forth by the American College of Cardiology/Society for Cardiac Angiography and Intervention.[1] ICA images were transmitted to independent masked readers at the CDCC, who evaluated ICA to determine culprit lesions, segments and vessels using an 18-segment Society of Cardiovascular Computed Tomography (SCCT) model of the coronary tree.[2] The SCCT model was chosen for ICA evaluation in order to align with the same model used for CCTA measurements (Figure V-I).

The Rule Out Myocardial Infarction approach by employing a Computer Assisted Tomography (ROMICAT) definition was used to determine culprit lesions by ICA. In ACS patients with a single significant stenosis, this lesion was considered the culprit lesion. In ACS cases with ≥2 significant lesions, the culprit lesion was defined on the basis of ICA (by the most severely narrowed lesion, or the lesion with the most complex morphology, or both) and ECG (by distribution of ischemia).[3,4] In ambiguous cases or cases with multiple candidate culprits, a consensus reading with a second cardiologist was performed. All other lesions were deemed non-culprit lesions.

CCTA alignment of ICA-determined culprit lesions to CCTA precursors

Subsequent to CL CCTA analysis, ICA-identified culprit lesions were co-registered to the lesions (D.H. and F.Y.L.) by comparison of coronary segment coding and using distance from ostia and coronary vessel branch points as fiduciary landmarks. Un-blinded comparison of ICA and CCTA was allowed for alignment of discrepancies but not for reclassification of ACS.

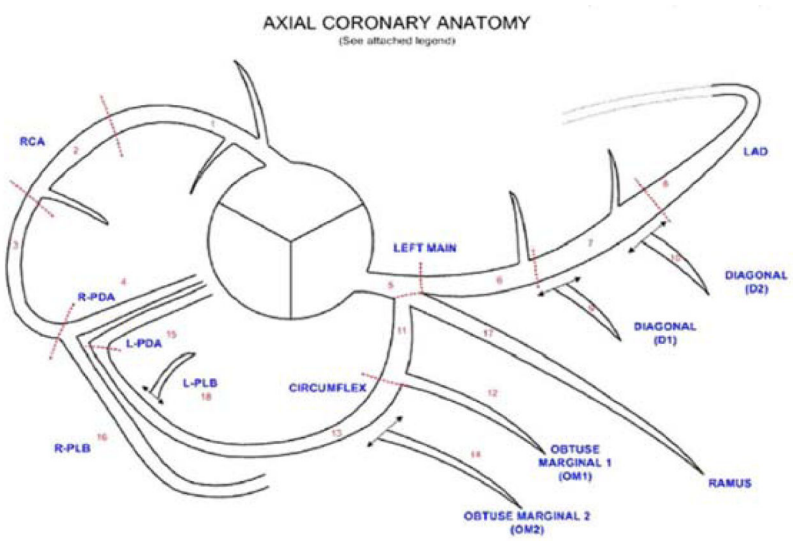

Figure V-1. Society of Cardiovascular CT 18-segment Coronary Tree

The same model was applied to both ICA and CCTA in order align baseline CCTAs with follow-up culprit lesions by ICA.

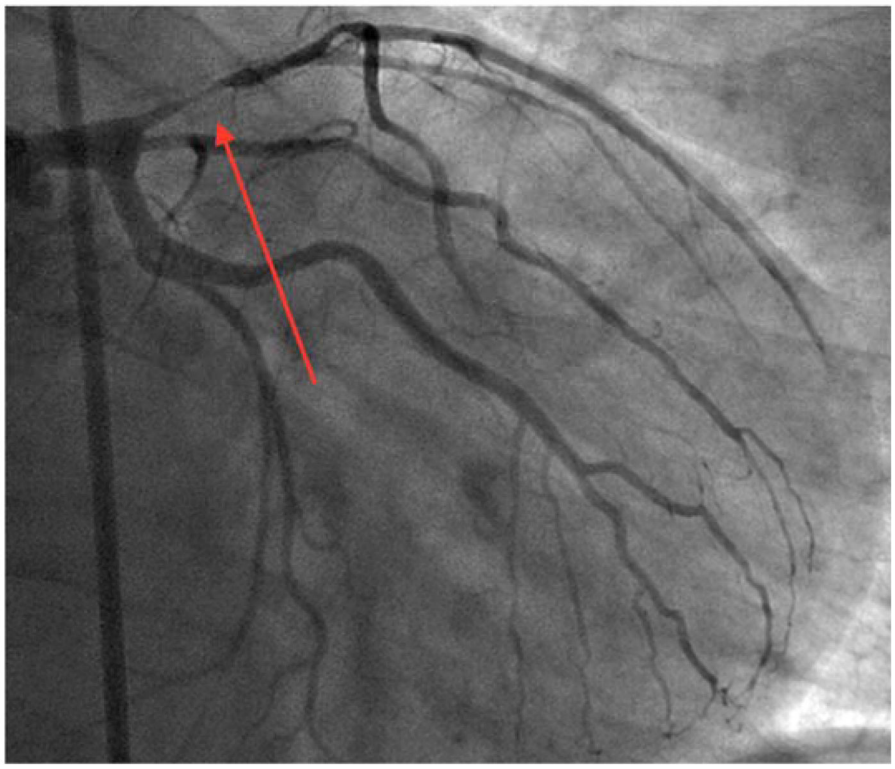

Figure V-2. Determination of culprit lesion by ICA

Blinded adjudication determined the presence of a culprit lesion in the proximal left anterior descending (LAD) artery by the presence of a single significant stenosis on the ICA at the

time of downstream ACS. Subsequently unblinded comparison was performed to align the culprit location to the culprit lesion precursor in the proximal LAD in the baseline CCTA.

References

1. Naidu SS, Rao SV, Blankenship J, et al. Clinical expert consensus statement on best practices in the cardiac catheterization laboratory: Society for Cardiovascular Angiography and Interventions. Catheterization and Cardiovascular Interventions. 2012; 80:456–64. [PubMed: 22434598]
2. Leipsic J, Abbara S, Achenbach S, et al. SCCT guidelines for the interpretation and reporting of coronary CT angiography: a report of the Society of Cardiovascular Computed Tomography Guidelines Committee. Journal of cardiovascular computed tomography. 2014; 8:342–58. [PubMed: 25301040]
3. Hoffmann U, Moselewski F, Nieman K, et al. Noninvasive assessment of plaque morphology and composition in culprit and stable lesions in acute coronary syndrome and stable lesions in stable angina by multidetector computed tomography. J Am Coll Cardiol. 2006; 47:1655–62. [PubMed: 16631006]
4. Ferencik M, Schlett CL, Ghoshhajra BB, et al. A computed tomography-based coronary lesion score to predict acute coronary syndrome among patients with acute chest pain and significant coronary stenosis on coronary computed tomographic angiogram. Am J Cardiol. 2012; 110:183–9. [PubMed: 22481015]

Appendix VI. CCTA definitions

CCTA acquisition and quality assurance

Baseline CCTA referral, performance, and site interpretation had been performed in accordance with each site's institutional policy prior to initiation of the ICONIC study.[1,2] Scans were performed using ≥64-detector row single- or dual-source scanners, with multiple vendors, using both prospective and retrospective gating. CCTA scan parameters including tube current (mA), tube voltage (kV), dose-length product and contrast dose were recorded by individual sites. Site-submitted DICOM files for cases and controls were transmitted to the CCTA imaging core lab.

The CCTA imaging core lab performed quantitative and qualitative measurements of CCTA utilizing semi-automated plaque analysis software (MEDIS QAngio CT Research Edition v2.1.9.1, Medis Medical Imaging Systems, Leiden, the Netherlands, Figure VI-I), with reconstructions at the smallest slice thickness (e.g., ~500 μm), as previously described.[3,4] Standard displays (e.g., width 740 Hounsfield Unit (HU), level 220 HU) were adjusted by contrast level of the aorta (155% and 65% mean luminal intensity of central aorta). The presence of atherosclerosis was defined as any tissue >1mm^2 within or adjacent to the lumen that can be discriminated from surrounding pericardial tissue, epicardial fat, or lumen; and identified in >2 planes.[5] Independent level III-experienced readers analyzed each CCTA on a per-segment level, masked to clinical and test results. Measurements were then summarized on a per-patient level.

Consistency for interobserver and intraobserver variability of total plaque volume and plaque composition was maintained with biweekly QC and QA compared to other core lab readers and intravascular ultrasound. The interobserver and intraobserver intraclass correlation for total plaque volume was 0.992 and 0.996 ($p<0.001$ respectively). The

interobserver and intraobserver intraclass correlation for plaque composition ranged from 0.95–0.99 (Table VI-1)

Per-segment basis

Segments classified by an 18-segment SCCT model were qualitatively evaluated for the presence and categorical stenosis severity of CAD.[1,6,7] Quantitative segment analysis was performed for length, vessel volume (VV, mm^3), lumen volume, and plaque volume (PV, mm^3).[8–10] Volumes of each plaque type were measured based on HU thresholds including: 1) calcified plaque (HU>350), 2) fibrous plaque (HU 131–350), 3) fibrofatty plaque (HU 31–130), and 4) necrotic core (HU −30-30).[3,4]

Per-lesion basis

Lesions, which did not necessarily conform to segment boundaries, were qualitatively evaluated for the following adverse plaque characteristics: 1) low attenuation plaque (LAP) defined by HU<30; 2) positive remodeling (PR), defined by remodeling index ≥1.1; 3) spotty calcification (SC) defined as a visually detectable calcification ≤3mm in any direction within a plaque, 4) napkin-ring sign, defined as a ringlike morphology of noncalcified plaque with a circumferential region of hyperattenuated plaque surrounding a region of hypoattenuation with HU<70 5) plaque composition as none, non-calcified (>70% non-calcified), mixed (30–70% non-calcified or calcified), and calcified (>70 calcified), 6) bifurcation as present if it was present within 5mm of the lesion, with no distinction between bifurcation and trifurcation, and 7) tortuosity, defined as positive if one >90-degree bend or three 45–90 degree curves were found using a 3-point angle within the lesion.[8,11–15] High-risk plaque (HRP) was defined as the presence within a coronary lesion of ≥2 features including PR, LAP, or SC.

Quantitative lesion analysis was performed for plaque and vessel lengths and volumes similar to the segment analysis. In addition, the maximally stenotic cross-section was measured for minimal luminal area, minimal and maximal plaque thickness, and plaque area. The site of maximal stenosis was chosen semi-automatically by the quantitative CT program using the minimal lumen area within a highlighted lesion with subsequent manual correction. Cross-sectional plaque burden was defined as plaque area at the maximally stenotic cross-section/vessel area at the maximal stenotic cross section × 100 (%). Stenosis severity was calculated in comparison to the normal reference vessel size, defined by an average of the 5 mm proximal to and 5 mm distal to the lesion boundaries with manual correction for to the nearest normal reference cross-section in the case of branch vessels and tandem lesions.[16] Luminal area was measured by planimetry and used to calculate the geometric mean diameter for estimates of diameter stenosis severity. The remodeling index was calculated in comparison to the proximal vessel area 5mm proximal to the lesion, again with manual correction for branch vessels and tandem lesions.[11]

Chronic total occlusions and patients with no plaque qualitatively identified on per-segment analysis could not undergo lesion measurements using QAngioCT but were assigned % diameter stenosis of 100% and 0% respectively.

Per-patient basis

After vessel volume (VV, mm^3) and plaque volume (PV, mm^3) of all coronary segments were obtained,[17] they were summated to generate PV and VV on a per-patient and per-lesion level. For all continuous per-lesion and per-segment variables, we calculated maxima, minima, and sums on a per-patient basis. For all categorical per-lesion and per-segment variables, we calculated counts and binary presence.

Mean plaque burden (PB) was defined as [(total PV/total VV) × 100] (%).[17] A segment involvement score was calculated, as we have previously described,[18] which summates the total number of coronary segments with any atherosclerotic plaque. A segment stenosis score was similarly calculated, with each coronary segment graded in ordinal fashion between 0–3 based upon the severity of stenosis, and summated to yield a total per-patient score.[18] Diffuseness of atherosclerosis was calculated as a % of the summed length of coronary lesions divided by the total vessel lengths.

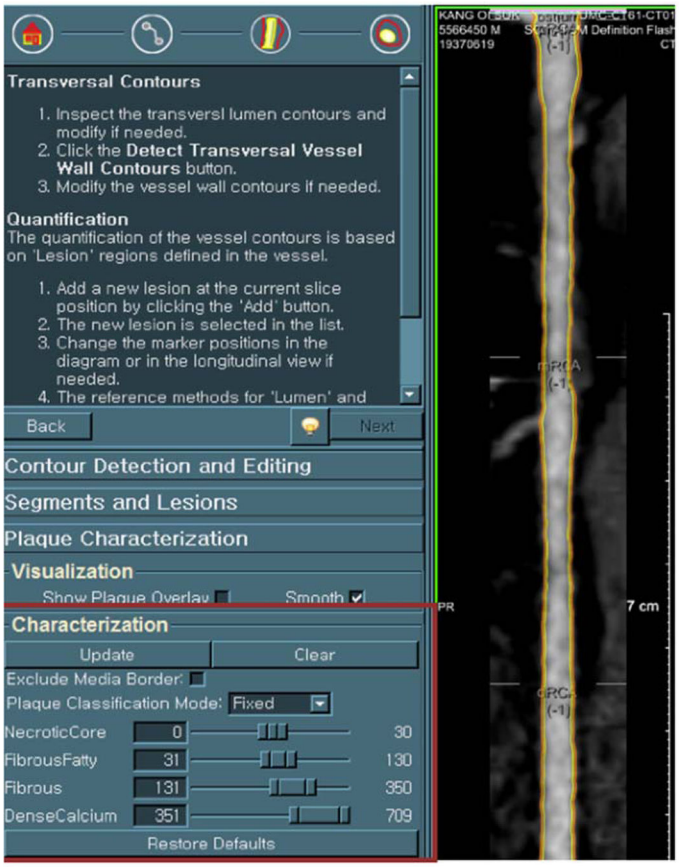

Figure VI-1.
Medis QAngio-CT measurement with center-plane reformat of coronary artery.

Table VI-1

CCTA Core Lab inter- and intra-observer variability with QAngio-CT

Inter	Interobserver ICC*	*P* value	Intraobserver ICC*	*P value*
Plaque volume	0.992	<0.0001	0.996	<0.001
Calcified PV	0.996	<0.0001	0.998	<0.001
Fibrous PV	0.969	<0.0001	0.992	<0.001
Fibro-Fatty PV	0.984	<0.0001	0.988	<0.001
Necrotic Core PV	0.946	<0.0001	0.996	<0.001

*ICC: Intra-class correlation coefficient

References

1. Raff GL, Abidov A, Achenbach S, et al. SCCT guidelines for the interpretation and reporting of coronary computed tomographic angiography. J Cardiovasc Comput Tomogr. 2009; 3:122–36. [PubMed: 19272853]
2. Abbara S, Arbab-Zadeh A, Callister TQ, et al. SCCT guidelines for performance of coronary computed tomographic angiography: a report of the Society of Cardiovascular Computed Tomography Guidelines Committee. J Cardiovasc Comput Tomogr. 2009; 3:190–204. [PubMed: 19409872]
3. Boogers MJ, Broersen A, van Velzen JE, et al. Automated quantification of coronary plaque with computed tomography: comparison with intravascular ultrasound using a dedicated registration algorithm for fusion-based quantification. Eur Heart J. 2012; 33:1007–16. [PubMed: 22285583]
4. Park HB, Lee BK, Shin S, et al. Clinical Feasibility of 3D Automated Coronary Atherosclerotic Plaque Quantification Algorithm on Coronary Computed Tomography Angiography: Comparison with Intravascular Ultrasound. Eur Radiol. 2015; 25:3073–83. [PubMed: 25994190]
5. Budoff MJ, Dowe D, Jollis JG, et al. Diagnostic performance of 64-multidetector row coronary computed tomographic angiography for evaluation of coronary artery stenosis in individuals without known coronary artery disease: results from the prospective multicenter ACCURACY (Assessment by Coronary Computed Tomographic Angiography of Individuals Undergoing Invasive Coronary Angiography) trial. J Am Coll Cardiol. 2008; 52:1724–32. [PubMed: 19007693]
6. Min JK, Shaw LJ, Devereux RB, et al. Prognostic value of multidetector coronary computed tomographic angiography for prediction of all-cause mortality. J Am Coll Cardiol. 2007; 50:1161–70. [PubMed: 17868808]
7. Pagali SR, Madaj P, Gupta M, et al. Interobserver variations of plaque severity score and segment stenosis score in coronary arteries using 64 slice multidetector computed tomography: a substudy of the ACCURACY trial. J Cardiovasc Comput Tomogr. 2010; 4:312–8. [PubMed: 20630819]
8. Motoyama S, Kondo T, Sarai M, et al. Multislice computed tomographic characteristics of coronary lesions in acute coronary syndromes. J Am Coll Cardiol. 2007; 50:319–26. [PubMed: 17659199]
9. Schlett CL, Ferencik M, Celeng C, et al. How to assess non-calcified plaque in CT angiography: delineation methods affect diagnostic accuracy of low-attenuation plaque by CT for lipid-core plaque in histology. Eur Heart J Cardiovasc Imaging. 2013; 14:1099–105. [PubMed: 23671211]
10. de Graaf MA, Broersen A, Kitslaar PH, et al. Automatic quantification and characterization of coronary atherosclerosis with computed tomography coronary angiography: cross-correlation with intravascular ultrasound virtual histology. Int J Cardiovasc Imaging. 2013; 29:1177–90. [PubMed: 23417447]
11. Motoyama S, Sarai M, Harigaya H, et al. Computed tomographic angiography characteristics of atherosclerotic plaques subsequently resulting in acute coronary syndrome. J Am Coll Cardiol. 2009; 54:49–57. [PubMed: 19555840]

12. Motoyama S, Kondo T, Anno H, et al. Atherosclerotic plaque characterization by 0. 5-mm-slice multislice computed tomographic imaging. Circ J. 2007; 71:363–6. [PubMed: 17322636]
13. Ehara S, Kobayashi Y, Yoshiyama M, et al. Spotty calcification typifies the culprit plaque in patients with acute myocardial infarction: an intravascular ultrasound study. Circulation. 2004; 110:3424–9. [PubMed: 15557374]
14. Maurovich-Horvat P, Schlett CL, Alkadhi H, et al. The napkin-ring sign indicates advanced atherosclerotic lesions in coronary CT angiography. JACC Cardiovascular imaging. 2012; 5:1243–52. [PubMed: 23236975]
15. Otsuka K, Fukuda S, Tanaka A, et al. Napkin-ring sign on coronary CT angiography for the prediction of acute coronary syndrome. JACC Cardiovascular imaging. 2013; 6:448–57. [PubMed: 23498679]
16. Stone GW, Maehara A, Lansky AJ, et al. A prospective natural-history study of coronary atherosclerosis. N Engl J Med. 2011; 364:226–35. [PubMed: 21247313]
17. Papadopoulou S-L, Neefjes LA, Garcia-Garcia HM, et al. Natural history of coronary atherosclerosis by multislice computed tomography. JACC: Cardiovascular Imaging. 2012; 5:S28–S37. [PubMed: 22421228]
18. Min JK, Shaw LJ, Devereux RB, et al. Prognostic value of multidetector coronary computed tomographic angiography for prediction of all-cause mortality. Journal of the American College of Cardiology. 2007; 50:1161–70. [PubMed: 17868808]

Appendix VII. Additional statistics

Table VII-1

Baseline clinical characteristics of the ICONIC study.

Variables	ACS Case (n= 234) N(%) or Mean±SD	Control (n= 234) N(%) or Mean±SD	P-value**
Age, year*	62.2 (11.5)	62.4 (10.4)	0.567
Male, %*	149 (63.7)	146 (62.4)	0.532
Risk factors*			
Hypertension, %	148 (63.2)	143 (61.1)	0.497
Dyslipidemia, %	129 (55.1)	123 (52.6)	0.477
Diabetes, %	46 (19.7)	74 (31.6)	<0.001
Smoking (current or past combined)	110 (47.0)	87 (37.2)	0.216
Premature family history CAD, %	94 (40.2)	87 (37.2)	0.174
CAD severity (site read)*			
None	15 (6.4)	28 (12.0)	0.101
Nonobstructive	47 (20.1)	91 (38.9)	
1-vessel obstructive	78 (33.3)	41 (17.5)	
2-vessel obstructive	35 (15.0)	37 (15.8)	
3-vessel/left main	48 (20.5)	37(15.8)	
Propensity Score	0.07(0.04)	0.07(0.04)	0.728
Race/Ethnicity			0.467
White	111 (47.9)	111 (47.4)	
East Asian	53 (22.6)	53 (22.6)	
Others	12 (5.1)	14 (6.0)	
Body Mass Index, kg/m2	27.6 (5.1)	27.2 (4.6)	0.537

Variables	ACS Case (n= 234) N(%) or Mean±SD	Control (n= 234) N(%) or Mean±SD	P-value**
Angina type, %			0.004
Asymptomatic, %	37 (15.8)	75 (32.1)	
Non-cardiac, %	28 (12.0)	32 (13.7)	
Atypical angina, %	94 (40.2)	83 (35.5)	
Typical angina, %	63 (26.9)	37 (15.8)	
Dyspnea, %	40 (17.1)	47 (20.1)	0.396
Medications			
Statin	96 (41)	84 (35.9)	0.211
ASA/Clopidogrel, %	93 (39.7)	86 (36.8)	0.710
Warfarin (Coumadin), %	9 (3.8)	12 (5.1)	0.564
ACE-I/ARB, %	32 (13.7)	38 (16.2)	0.475
Beta blocker, %	63 (26.9)	67 (28.6)	0.491
Nitrates, %	11 (4.7)	8 (3.4)	0.317
Lipid profile			
Total, mg/dl	193.1 (48.3)	186.3 (52.2)	0.317
LDL, mg/dl	117.7 (41.7)	112.5 (37.3)	0.434
HDL, mg/dl	47.8 (13.6)	46.7 (15.2)	0.353
Triglycerides, mg/dl	118.6 (105.0)	132.0 (83.0)	0.269
Coronary Artery Calcium Score (site read)			0.241
0	29 (12)	30 (13)	
1–100	36 (15)	41 (18)	
101–400	39 (17)	24 (18)	
>400	44 (19)	31 (13)	
Follow-up duration, year	3.9 (2.7)	3.8 (2.4)	0.971
Interval revascularization	118 (50.4)	55 (23.5)	<0.001
Time to any revascularization	0.8 (1.4)	0.6 (0.8)	0.033
ACS due to revascularization	N/A	N/A	N/A
ACM post ACS	16 (6.8)	N/A	N/A
CCTA Scanner Type			0.004
64 slice, %	101 (43.2)	91 (38.9)	
Dual source, %	78 (33.3)	89 (38.0)	
Other, %	38 (16.2)	31 (13.2)	
Contrast dose	89 (16)	87 (14)	0.10
Prospective Gating	30 (12.8)	6 (2.6)	0.56
ma	673.1 (232.8)	678.4 (200.6)	0.12
kV	118.5 (29.2)	115.5 (8.9)	0.20
DLP	784.6 (438.7)	702.3 (445)	0.28
Dose in millisieverts	11.0 (6.1)	9.8 (6.2)	0.28
Case Characteristics			

Variables	ACS Case (n= 234) N(%) or Mean±SD	Control (n= 234) N(%) or Mean±SD	P-value**
STEMI	40 (17.1)	N/A	N/A
NSTEMI	114 (48.7)	N/A	N/A
MI, non-specified	6 (2.6)	N/A	N/A
UA	74 (31.6)	N/A	N/A
Time to first event			
< 2 weeks	76 (32.5)	N/A	N/A
2wks – 6 months	63 (26.9)	N/A	N/A
6 mo–1 year	21 (9.0)	N/A	N/A
1–2 year	26 (11.1)	N/A	N/A
≥ 2 years	48 (20.5)	N/A	N/A
MI location by EKG			
Anterior	25 (10.7)	N/A	N/A
Inferior	17 (7.3)	N/A	N/A
Posterolateral	13 (5.6)	N/A	N/A
Indeterminate/other	166 (70.9)	N/A	N/A

*components of the propensity score

**Paired comparisons with Wilcoxon rank-sum for categorical and paired t-test for continuous

CAD: coronary artery disease.

Table VII-2

Per-patient comparison of additional baseline plaque characteristics.

Variables	ACS Case (n= 234) N(%) or Mean±SD	Control (n= 234) N(%) or Mean±SD	P-value**
Segment Stenosis Score (0–48)	6.8 (4.9)	6.5 (5.3)	0.324
Segment Involvement Score (0–16)	5.3 (3.1)	5 (3.4)	0.373
Presence of napkin ring sign, n (%)	14 (6)	9 (3.8)	0.400

Table VII-3

Per-patient comparison in baseline CCTA restricted to those who underwent interval PCI

Atherosclerotic feature	ACS underwent interval revasc (n= 118) N(%) or mean±SD	Control underwent interval revasc (n= 55) N(%) or mean±SD	p-value
Age, year*	62.2 (10.8)	65.5 (8.9)	0.097
Male, %*	81 (68.6)	36 (65.5)	0.676
Case Characteristics			
STEMI	27 (22.9)		
NSTEMI	57 (48.3)		
MI, non-specified	5 (4.2)		
UA	29 (24.6)		

Atherosclerotic feature	ACS underwent interval revasc (n= 118) N(%) or mean±SD	Control underwent interval revasc (n= 55) N(%) or mean±SD	p-value
Number of total lesions	4.2 (2.5)	5.1 (2.5)	0.022
Diameter stenosis, %	45.1±23.6	47.7±20.5	0.550
%DS ≥50%	42 (35.6)	21 (38.2)	0.742
%DS ≥70%	13 (11)	7 (12.7)	0.743
Area stenosis, %	64.3±24.9	68.5±19.7	0.549
Minimum luminal area, mm^2	2.1±1.6	1.7±1.0	0.355
Minimum luminal diameter, mm	1.3±0.6	1.2±0.5	0.577
CAD severity by number of vessels			0.004
None	5 (4.2)	1 (1.8)	
Nonobstructive (≤50% DS)	11 (9.3)	15 (27.3)	
1VD	53 (44.9)	13 (23.6)	
2VD	36 (30.5)	15 (27.3)	
3VD/left main disease	13 (11)	11 (20)	
Total plaque volume, mm^3	311.3±295.3	464.2±346.7	0.003
Calcified, mm^3	115.2±152.7	183.5±229.5	0.031
Fibrous, mm^3	138.2±128.9	187.6±142.4	0.015
Fibro-fatty, mm^3	52.8±63	84.4±94.3	0.075
Necrotic core, mm^3	5.2±11.5	8.7±11.9	0.039
Fibro-fatty + necrotic core, mm^3	58±69.4	93.1±103.2	0.077
Noncalcified, mm^3	196.2±176.1	280.7±217.6	0.014
Composition by % vessel volume			
% Calcified	5.0±6.8	6.8±7.1	0.031
% Fibrous	5.7±4.6	7.4±4.9	0.025
% Fibro-fatty	2.2±2.3	3.4±3.7	0.119
% Necrotic core	0.2±0.7	0.3±0.5	0.045
% Fibro-fatty + necrotic core	2.4±2.7	3.7±4	0.099
% Noncalcified volume	8.1±6.3	11.1±7.9	0.023
Mean plaque burden, %	13.1±11.1	17.9±10.8	0.003
Diffuseness, %	25.8±19.4	33.3±18.0	0.163
Adverse plaque characteristics			
Bifurcation, number of lesions	2.3±1.6	2.9±1.8	0.067
Tortuous vessels, number of lesions	0.1±0.4	0.1±0.4	0.459
High-risk plaque present	72 (61)	28 (50.9)	0.210
Low-attenuation plaque present	58 (49.2)	28 (50.9)	0.830
Positive remodeling present	107 (90.7)	50 (90.9)	0.961
Spotty calcification present	44 (37.3)	11 (20)	0.023

Table VII-4

Comparison of ACS case patients with and without aligned culprit lesions

Atherosclerotic feature	ACS with culprit lesion (n= 162) N(%) or mean±SD	ACS without identified culprit (n= 72) N(%) or mean±SD	p-value
Age, year*	61.5±11.3	63.8±11.9	0.245
Male, %*	108 (66.7)	41 (56.9)	0.153
Case Characteristics			0.075
STEMI	32 (19.8)	8 (11.1)	
NSTEMI	70 (43.2)	44 (61.1)	
MI, non-specified	5 (3.1)	1 (1.4)	
UA	55 (34)	19 (26.4)	
Number of total lesions	4.3±2.6	3.2±2.3	0.006
Diameter stenosis, %	46.3±24.8	39.4±29.3	0.017
%DS ≥50%			
%DS ≥70%			
Area stenosis, %	65.1±24.9	54.8±31	0.017
Minimum luminal area, mm^2	2.1±1.8	2.8±2.6	0.174
Minimum luminal diameter, mm	1.3±0.6	1.5±0.8	0.139
CAD severity by number of vessels			0.059
None	6 (3.7)	9 (12.5)	
Nonobstructive (≤50% DS)	15 (9.3)	6 (8.3)	
1VD	71 (43.8)	33 (45.8)	
2VD	54 (33.3)	15 (20.8)	
3VD/left main disease	16 (9.9)	9 (12.5)	
Total plaque volume, mm^3	312.4±329.3	238.5±250	0.086
Calcified, mm^3	106.4±143.7	78.2±115.9	0.045
Fibrous, mm^3	137.8±139.7	102.1±108.4	0.046
Fibro-fatty, mm^3	61.7±92.4	52±68.7	0.409
Necrotic core, mm^3	6.5±13.4	6.4±15.3	0.732
Fibro-fatty + necrotic core, mm^3	68.2±101.5	58.4±80.5	0.4
Noncalcified, mm^3	206±221.3	160.5±171	0.1
Composition by % vessel volume			
% Calcified	4.5±6.1	3.3±5.1	0.027
% Fibrous	5.6±4.7	4.2±4.1	0.019
% Fibro-fatty	2.4±3.1	2.1±3	0.332
% Necrotic core	0.3±0.7	0.3±0.6	0.641
% Fibro-fatty + necrotic core	2.7±3.5	2.4±3.5	0.322
% Noncalcified volume	8.3±7.4	6.6±6.8	0.049
Mean plaque burden, %	12.8±11.2	9.8±10	0.035
Diffuseness, %	0.3±0.2	0.2±0.2	0.005

Atherosclerotic feature	ACS with culprit lesion (n= 162) N(%) or mean±SD	ACS without identified culprit (n= 72) N(%) or mean±SD	p-value
Adverse plaque characteristics			
Bifurcation, number of lesions	2.4±1.6	1.9±1.4	0.032
Tortuous vessels, number of lesions	0.1±0.3	0.1±0.3	0.321
High-risk plaque present	89 (54.9)	33 (45.8)	0.198
Low-attenuation plaque present	72 (44.4)	29 (40.3)	0.552
Positive remodeling present	148 (91.4)	57 (79.2)	0.009
Spotty calcification present	53 (32.7)	19 (26.4)	0.333

Appendix VIII. Differences between nested case-control and non-analyzed eligible cohort patients

After exclusion of prior CAD and death without antecedent ACS, there were 583 site-adjudicated ACS events and 22,217 non-events. After exclusion of cases that did not meet criteria for core-lab adjudicated ACS, had ACS attributable to segment revascularized after the baseline CCTA, or lacked CCTA measurements, and after matching of controls, there remained 234 core lab adjudicated analyzable cases and controls. The comparison of analyzed cases and controls can be seen in Appendix VII.

Those analyzed in the final ICONIC cohort did not differ from excluded candidate ACS events by propensity score, race, CAD severity or interval revascularization (Table VIII-I). However, there were significant differences in some clinical predictors including lower rates of diabetes and higher rates of family history, current smoking, and angina severity, and baseline statin usage.

As expected by the propensity-matched study design, analyzed non-events were significantly higher risk compared to excluded non-events by propensity score, by factors included in the propensity score including risk factors and CAD severity, and by interval revascularization (Table VIII-I). Correspondingly, cardiac medication usage was generally higher in analyzed than excluded non-events.

Table VIII-1

Difference between analyzed and excluded patients, by ACS event status

	Eligible Site-adjudicated ACS events N = 583			Eligible Site-adjudicated non-events N = 22217		
	Analyzed N=234 N(%) or Mean±SD	Excluded N = 349 N(%) or Mean±SD	P-value	Analyzed N = 234 N(%) or Mean±SD	Excluded N = 21,983 N(%) or Mean±SD	P-value
Propensity Score	0.07±0.04	0.07±0.05	0.447	0.07±0.04	0.03±0.03	<0.001
Age	62.2±11.5	62.7±11.4	0.851	62.4±10.4	56.4±11.8	<0.001
Women	36.3%	35.5%	0.845	37.6%	45.2%	0.020

	Eligible Site-adjudicated ACS events N = 583			Eligible Site-adjudicated non-events N = 22217		
	Analyzed N=234 N(%) or Mean±SD	Excluded N = 349 N(%) or Mean±SD	P-value	Analyzed N = 234 N(%) or Mean±SD	Excluded N = 21,983 N(%) or Mean±SD	P-value
CAD RF:						
Hypertension	63.8%	61.5%	0.569	61.1%	47.7%	<0.001
Hyperlipidemia	55.6%	53.0%	0.542	52.6%	49.0%	0.281
Diabetes	19.7%	28.5%	0.016	31.6%	16.4%	<0.001
FH	41.2%	31.5%	0.017	37.3%	30.9%	0.033
Current smoking	30.8%	22.1%	0.018	23.5%	17.5%	0.015
CAD severity:			0.446			<0.001
None	6.7%	10.3%		12.0%	42.0%	
Nonobs	21.1%	21.8%		15.8%	37.8%	
1vd	35.0%	31.5%		38.9%	12.3%	
2vd	15.7%	18.2%		17.5%	4.8%	
3vd/LM	21.5%	18.2%		15.8%	3.2%	
Race:			0.113			0.363
White	63.3%	69.0%		62.4%	57.1%	
East Asian	29.9%	28.3%		29.8%	34.4%	
Other	6.8%	2.7%		7.9%	8.5%	
Angina type:			0.009			0.066
Asymptomatic	16.7%	28.5%		33.0%	39.3%	
Noncardiac	11.7%	7.5%		14.1%	11.7%	
Atypical angina	43.2%	39.0%		36.6%	37.3%	
Typical angina	28.4%	24.9%		16.3%	11.8%	
Dyspnea	21.9%	19.3%	0.492	26.3%	21.5%	0.123
Medications:						
Statins	58.5%	42.0%	0.001	50.6%	32.5%	<0.001
ASA/Clopidogrel	53.1%	47.7%	0.256	48.9%	34.3%	<0.001
Warfarin	8.6%	10.4%	0.616	11.0%	5.4%	0.011
ACEI/ARB	37.9%	38.8%	0.859	35.8%	27.5%	0.015
Beta blocker	36.2%	32.2%	0.387	38.1%	29.5%	0.013
Nitrates	8.9%	9.4%	0.874	6.3%	9.2%	0.260
Follow-up (years)	3.9±2.7	4.3±2.6	0.034	3.8±2.4	3.3±2.0	0.007
Interval revasc	24.8%	28.9%	0.270	23.5%	7.7%	<0.001

PERSPECTIVES

Competency in Medical Knowledge

Although acute coronary syndrome is associated with stenosis severity, most precursors of ACS cases and culprit lesions are non-obstructive. Noninvasive plaque evaluation, including CCTA evaluation of high-risk plaque, plaque composition, and cross-sectional plaque burden, independently predict first ACS beyond stenosis severity and aggregate plaque burden.

Translational Outlook

Quantitative measurement of plaque composition, as well as high-risk plaque evaluation and cross-sectional plaque burden, should be investigated for risk stratification in future cohort studies.

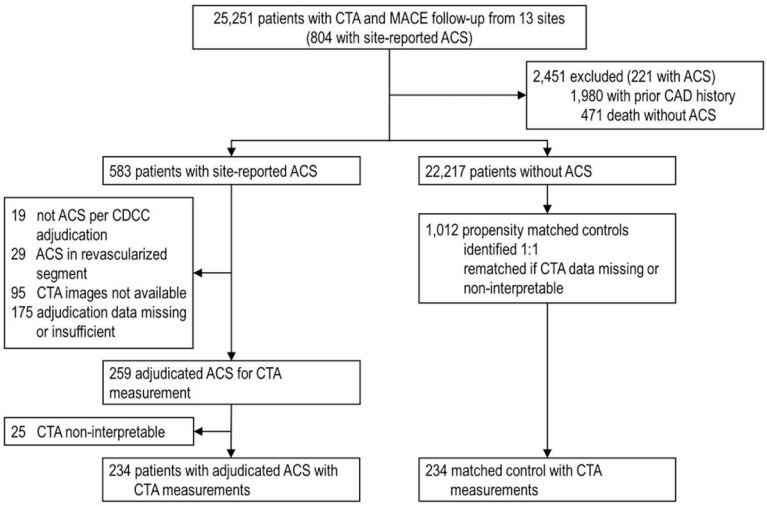

Figure 1. CONSORT Diagram for the ICONIC study

ACS, acute coronary syndrome; CAD, coronary artery disease; CDCC, The Clinical and Data Coordinating Center; CTA, coronary computed tomography angiography; MACE, major adverse cardiac event

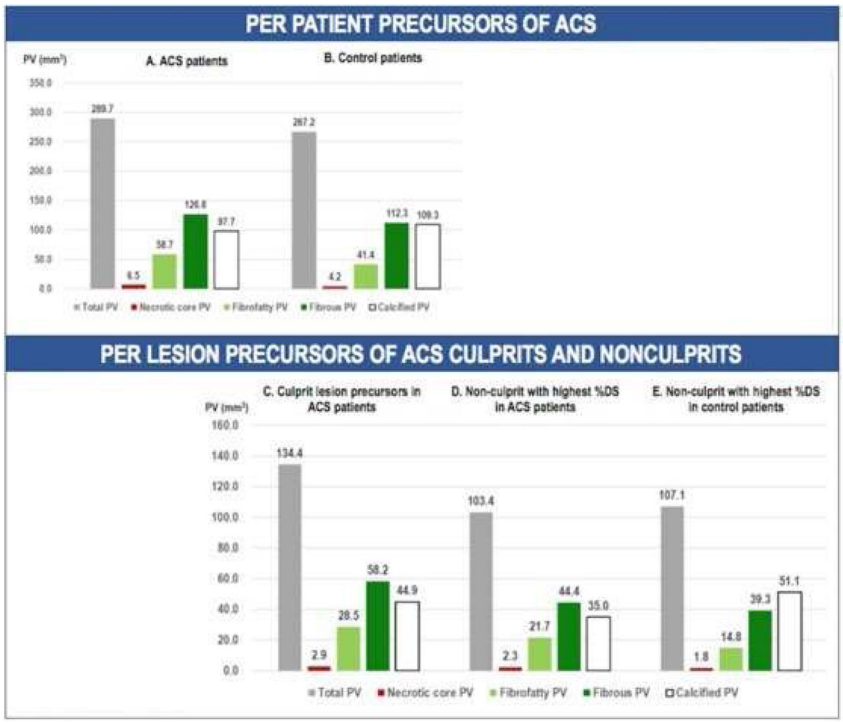

Central Illustration. Precursors of ACS and controls as identified by CCTA

A. Adjudicated first ACS cases with CCTA measurements (n = 234) of a nested case-control cohort of 25,251 patients undergoing CCTA exhibit elevated fibro-fatty and necrotic core volumes (65.2 ± 95.4 mm3); 34.6% exhibit diameter stenosis ≥50% and 52.1% exhibit high-risk plaque. **B**. Non-event controls propensity matched by demographics, risk factors, and number of obstructive vessels by CCTA exhibit lesser fibro-fatty and necrotic core volumes (45.6 ± 68.8, multivariate adjusted p = 0.008) with no difference in calcified or total plaque volumes (p = NS for all); %DS and HRP are significantly decreased in control patients (p<0.05 for all). **C**. Culprit lesion precursors exhibit elevated fibro-fatty and necrotic core volumes (31.32 ± 55.5 mm3). **D**. Within-patient controls, using the non-culprit with the highest baseline %DS, exhibit lesser total plaque and necrotic core volumes (p<0.05 for both). **E**. Between-patient controls, using the lesion with the highest %DS in the control patient, exhibit lesser non-calcified plaque components (p = 0.04), but no decrease in calcified plaque volume (p = NS). ACS, acute coronary syndrome; CCTA, coronary computed tomographic angiography; %DS, percent diameter stenosis; HRP, high-risk plaque; NS, nonsignificant.

Table 1

CCTA findings in patient-level analysis

Atherosclerotic feature	ACS (n= 234) N(%) or mean±SD	Control (n= 234) N(%) or mean±SD	p-value
Number of total lesions	3.9 (2.5)	3.7 (2.7)	0.400
Diameter stenosis, %	44.2±26.4	33.7±22.0	<0.001
%DS ≥50%	81 (34.6)	45 (19.2)	<0.001
%DS ≥70%	30 (12.8)	12 (5.1)	0.007
Area stenosis, %	61.9±27.2	51.2±27.9	<0.001
Minimum luminal area, mm^2	2.3±2.1	2.6±1.9	0.014
Minimum luminal diameter, mm	1.3±0.7	1.5±0.6	0.004
CAD severity by number of vessels			0.020
None	15 (6.4)	34 (14.5)	
Non-obstructive (≤50% DS)	104 (44.4)	91 (38.9)	
1-vessel disease	69 (29.5)	59 (25.2)	
2-vessel disease	25 (10.7)	21 (9.0)	
3-vessel/left main disease	21(9.0)	29 (12.4)	
Total plaque volume, mm^3	289.7±308.4	267.2±285.7	0.321
Calcified, mm^3	97.7±136.1	109.3±164.0	0.389
Fibrous, mm^3	126.8±131.6	112.3±119.3	0.137
Fibro-fatty, mm^3	58.7±85.8	41.4±62.2	0.009
Necrotic core, mm^3	6.5±14.0	4.2±8.8	0.026
Fibro-fatty + necrotic core, mm^3	65.2±95.4	45.6±68.8	0.008
Noncalcified, mm^3	192.0±207.8	157.9±173.6	0.030
Composition by % vessel volume			
% Calcified	4.1±5.9	4.5±6.2	0.709
% Fibrous	5.2±4.6	4.5±6.2	0.067
% Fibro-fatty	2.3±3.0	1.7±2.5	0.011
% Necrotic core	0.3±0.7	0.2±0.4	0.039
% Fibro-fatty + necrotic core	2.6±3.5	1.9±2.7	0.012
% Noncalcified volume	7.8±7.2	6.5±6.7	0.020
Mean plaque burden, %	11.9±10.9	11.0±10.7	0.152
Max cross-sectional plaque burden, %	66.1±25.8	56.5±28.7	<0.001
Diffuseness, %	25.8±19.4	22.3±19.2	0.030
Adverse plaque characteristics			
Bifurcation, # of lesions	2.3±1.6	2.1±1.7	0.218
Tortuous vessels, # of lesions	0.08±0.34	0.05±0.28	0.477
High-risk plaque present	122 (52.1)	78 (33.3)	0.003
Low-attenuation plaque present	101 (43.2)	64 (27.4)	<0.001
Positive remodeling present	205 (87.6)	187 (79.9)	0.026

Atherosclerotic feature	ACS (n= 234) N(%) or mean±SD	Control (n= 234) N(%) or mean±SD	p-value
Spotty calcification present	72 (30.8)	47 (20.1)	0.013

ACS, acute coronary syndrome; CAD, coronary artery disease; %DS, diameter stenosis; HRP, high-risk plaque; LAP, low-attenuation plaque; PR, positive remodeling; PV, plaque volume; SC, spotty calcification; SD, standard deviation

Table 2

Per-patient Multivariate Marginal Cox Model Predicting Acute Coronary Syndrome

Atherosclerotic feature	Hazard Ratio (95% Confidence Interval)*	P
Highest % diameter stenosis severity, per %	1.010 (1.005, 1.015)	0.002
Presence of ≥50% diameter stenosis	1.437 (0.948, 2.179)	0.088
Presence of ≥70% diameter stenosis	1.536 (1.141, 2.067)	0.005
Plaque volume, per mm^3	1.000 (0.999, 1.000)	0.792
Calcified	0.999 (0.998, 1.000)	0.092
Fibrous	1.000 (0.999, 1.001)	0.941
Fibro-fatty	1.002 (1.000, 1.004)	0.048
Necrotic core	1.013 (1.003, 1.022)	0.009
Fibro-fatty and necrotic core	1.002 (1.000, 1.003)	0.037
Non-calcified	1.000 (1.000, 1.001)	0.352
Mean plaque burden, %	1.005 (0.997, 1.013)	0.209
Max cross-sectional plaque burden, %	1.008 (1.003, 1.013)	0.003
Diffuseness, per %	1.146 (0.622, 2.111)	0.662
High-risk plaque present	1.593 (1.219, 2.082)	0.001
Low-attenuation plaque present	1.378 (1.051, 1.805)	0.020
Positive remodeling present	1.401 (0.955, 2.056)	0.085
Spotty calcification present	1.543 (1.169, 2.037)	0.002

*Adjusted for angina severity and interval revascularization

J Am Coll Cardiol. Author manuscript; available in PMC 2019 June 05.

Table 3

Lesion level analysis for identification of culprit lesion precursors

	Culprit lesion precursor (n=129)	Within-patient All non-culprits in ACS patients (n=479)			Within-patient Non-culprit with highest %DS in ACS patients (n=118)			Between-patient Lesion with highest %DS in control patient (n=129)		
	N (%) or mean±SD	N (%) or mean±SD	Hazard ratio† (95% CI)	P	N (%) or mean ±SD	Hazard ratio† (95% CI)	P	N (%) or mean ±SD	Hazard ratio† (95% CI)	P
% diameter stenosis	38.27±20.97	26.23±18.02	1.023 (1.015, 1.031)	<0.001	42.64±22.23	1.002 (0.994, 1.011)	0.612	37.04±20.63	1.001 (0.992, 1.010)	0.898
% DS ≥ 50%	32 (24.81)	41 (6.68)	2.813 (1.736, 4.558)	<0.001	31 (26.27)	1.256 (0.796, 1.982)	0.328	27 (20.93)	1.086 (0.682, 1.729)	0.727
% DS ≥ 70%	6 (4.65)	11 (1.25)	1.717 (0.678, 4.350)	0.254	11 (9.32)	0.607 (0.227, 1.622)	0.319	8 (6.20)	0.684 (0.268, 1.746)	0.427
Lesion length, mm	35.90±21.66	23.71±15.90	1.021 (1.013, 1.029)	<0.001	30.55±17.63	1.010 (1.001, 1.018)	0.029	29.36±21.71	1.004 (0.997, 1.011)	0.225
Plaque volume, mm^3	134.4±141.50	61.75±113.07	1.002 (1.001, 1.003)	<0.001	103.44±160.55	1.001 (1.000, 1.002)	0.030	107.11±125.80	1.000 (0.999, 1.002)	0.590
Calcified	44.88±60.29	21.18±45.78	1.004 (1.001, 1.006)	0.002	35.0±56.89	1.002 (1.000, 1.004)	0.077	51.07±83.89	0.998 (0.996, 1.001)	0.137
Fibrous	58.22±62.39	27.49±46.47	1.005 (1.002, 1.007)	<0.001	44.38±60.78	1.002 (0.999, 1.005)	0.108	39.31±47.11	1.002 (0.999, 1.005)	0.154
Fibro-fatty	28.47±50.18	11.99±34.08	1.007 (1.003, 1.010)	<0.001	21.71±55.67	1.003 (0.999, 1.007)	0.124	14.80±26.29	1.006 (1.002, 1.010)	0.006
Necrotic core	2.85±9.27	1.09±4.20	1.029 (1.018, 1.040)	<0.001	2.28±6.86	1.014 (1.001, 1.027)	0.042	1.75±4.71	1.012 (1.002, 1.022)	0.021
FF and NC	31.32±55.5	13.08±37.28	1.006 (1.003, 1.009)	<0.001	23.99±60.5	1.003 (0.999, 1.007)	0.119	16.55±29.96	1.005 (1.001, 1.008)	0.006
Non-calcified	89.51±107.36	40.55±77.27	1.003 (1.002, 1.005)	<0.001	68.34±114.82	1.002 (1.000, 1.003)	0.066	55.85±67.15	1.002 (1.000, 1.004)	0.042
Mean plaque burden, %	27.12±13.40	19.67±11.5	1.045 (1.032, 1.059)	<0.001	24.52±11.36	1.028 (1.011, 1.045)	0.001	25.42±14.75	1.003 (0.989, 1.017)	0.680
Max plaque burden, %	62.54 ±22.38	50.70±20.38	1.027 (1.018, 1.035)	<0.001	63.24±21.31	1.008 (1.000, 1.016)	0.050	57.84±27.83	1.003 (0.996, 1.010)	0.415
High-risk plaque	40 (31.01)	95 (19.83)	1.954 (1.317, 2.899)	0.001	36 (30.51)	1.239 (0.841, 1.827)	0.279	23 (17.83)	1.542 (1.105, 2.153)	0.011
Low-attenuation plaque	31 (24.03)	68 (14.20)	1.805 (1.198, 2.721)	0.005	28 (23.73)	1.085 (0.696, 1.693)	0.718	22 (17.05)	1.223 (0.840, 1.780)	0.294
Positive remodeling	99 (76.74)	379 (79.12)	1.048 (0.675, 1.628)	0.835	87 (73.73)	1.202 (0.743, 1.946)	0.453	73 (56.59)	2.031 (1.306, 3.160)	0.002
Spotty calcification	23 (17.83)	62 (12.94)	1.702 (1.064, 2.722)	0.026	18 (15.25)	1.506 (0.955, 2.375)	0.078	13 (10.08)	1.763 (1.241, 2.503)	0.002

*Eleven patients had measurements only for the culprit lesion and lacked a within-patient comparator.

†Adjusted for angina severity and interval revascularization.

%DS, % diameter stenosis; ACS, acute coronary syndrome; CI, confidence interval; FF, fibro-fatty; NC, necrotic core